University of Stavanger

Faculty of Science and Technology

MASTER'S THESIS

Study program/ Specialization: Petroleum Engineering/ Petroleum Geosciences Engineering	Fall semester, 2012 Open
Writer: Karina del R. Gil González	…… (Writer's signature)
Faculty supervisor: Dr Christopher Townsend External supervisor(s): Dr Christopher Townsend	
Title of thesis: 3D Geological Modelling of Kilve Beach SW England: normally faulted Liassic limestones and shales.	
Credits (ECTS): 30	
Key words: Normal Fault, Fault Zone, Major and Minor Structures, Lower Liassic age.	Pages: 84 + enclosure: 0…… Stavanger, 02.01.2013

Abstract

This study is based on the outcrops examples on Kilve Beach area, which is the onshore continuation of the Bristol Channel Basin, South of England, U.K. Kilve is a fault zone going into Lower Jurassic age limestones and mudrocks. The faults are well exposed on the Limestone bedding and related with the development of the Bristol Channel Basin during the Mesozoic (**Beach, 1989**). None of the Faults described on this project have showed evidence of strike-slip or reverse-reactivation that occurred in the Bristol Channel during the Tertiary (Beach, 1989).

The interpretation and understanding of the faults & horizons geometries are based on measurements, photographs, maps and GPS data taken on the field.

The localities were divided in three (Kilve Pill, Major fault 1 (Syncline 1) and After Red House or Major Fault 2 (Syncline 2)) in order to make a small scale interpretation due to the quality of the exposure. Two master faults have been identified as Normal presenting E-W striking with dip variable depending on the localities.

The three localities studied were dominated by E-W striking normal faults. The beddings exposed on the beach and cliff section consist of limestone and organic-rich shale interbedded. In general the dipping of these beddings was towards to the South-west.

The stratigraphic sequences and structural data were measured in the area and loaded in the *Petrel* ™ software to build a 3D geological model. 18 faults were interpreted on the outcrops, only 11 faults were included in the model (excluding the small reverse faults and those exposed only in the cliff section). The results show a good matching between the faults and horizons in the photographs digitized, also with the interpretations done in the field. The normal and reverse faults and horizons presented the same behaviour as well as those which were interpreted previously.

In addition, facies (i.e. sand and shale), petrophysical (i.e. porosity) and fluid properties (i.e. water saturation) were generated to get the volume calculations.

The structural model built in this study, may be used to improve the understanding of the large number of fields in the North Sea, which its developments are linked to the fault behaviour.

INDEX OF CONTENTS

1 Introduction 10

1.1 Study Area 11

1.2 Objectives 12

1.3 Previous works 12

2 Geological Context 15

2.1 Outcrop Structural Review 17

2.2 Outcrop Stratigraphy Review 17

3 Fault Description: Theory review 21

4 Measurements and Notation 24

5 Data Collection and field Observations 26

5.1 Outcrop data 26

5.1.1 Locality 1 (Kilve Pill) 29

5.1.2 Locality 2 (2 Major Structural Elements –F5-Syncline1 and F12) 37

5.1.3 Locality 3 (F15- Syncline 2) 42

6 Geological Modeling Process 48

6.1 Images Geo-referencing 48

6.2 Surface reference data 51

6.3 Structural Framework 56

6.4 Fault diagnosis 58

6.5 Model Segmentation 61

6.6 Zone Properties and Layering Process 64

6.7 Property Modeling 67

6.7.1 Geometrical Modeling 67

6.7.2 Facies Modelling 67

6.7.3 Petrophysical Modeling 69
6.7.4 Contacts and Volumens 69
7 Discussions 73
8 Conclusions 76
9 Recommendations for further work 77
10 References 78
10.1 Maps References 82
10.2 Manual references 82
11 Appendix 83
11.1 Raw data collected-GPS points 83
11.2 Fault data collected on the cliff section 84

INDEX OF FIGURES

FIGURE 1.1 *COMBINATION OF TOPOGRAPHIC MAP OF THE SOUTHWEST OF ENGLAND AND SATELLITE IMAGE, SHOWING THE LOCATION OF KILVE BEACH AND THE THREE LOCALITIES WHERE THE FIELDWORK WAS CARRIED OUT. BASED ON A SMALL PART OF ORDNANCE SURVEY FROM ANQUET MAPS 2011, ORIGINALLY 1:25,000 SCALES.* 14

FIGURE 2.1 *STRATIGRAPHIC CORRELATION OF THE LOWER LIASSIC EXPOSURE AT KILVE BEACH, COMPARED TO PUBLISHED ACCOUNTS (MODIFIED BY BRODAHL, E. (1993) AND KELLY ET AL, 1998)*.....18

FIGURE 2.2 *OUTCROP AND SUBCROP LIAS GROUP IN ENGLAND AND WALES SHOWING THE KILVE LOCATION AND MAIN SEDIMENTARY BASIN. AFTER COX ET AL. (1999) AND SIMMS ET AL.(2004)* ..19

FIGURE 2.3 *MAJOR GEOLOGICAL FEATURES OF SOUTH WALES AND THE BRISTOL CHANNEL BASED ON BRITISH GEOLOGICAL SURVEY MAPS AND TAPPIN ET AL. (1994). A = VARISCAN FRONT THRUST, B = CENTRAL BRISTOL CHANNEL FAULT ZONE.*.....20

FIGURE 3.1 *EXAMPLE OF NORMAL FAULT WITH ITS DIMENSIONS* 21

FIGURE 3.2 *FIELD EXAMPLE SHOWING MAYOR AND MINOR STRUCTURES.*.....23

FIGURE 4.1 TOOLS USED IN THE MEASUREMENTS AND NOTATION 25

FIGURE 5.1 A) *PROFILE ON THE CLIFF AND B) THE BEACH EXPOSURE, FAULTS INTERPRETED (2 MAJOR FAULTS (IN RED), INTO THE MINORS FAULTS ARE 2-REVERSE FAULTS (IN WHITE) AND 9 NORMAL FAULTS (IN YELLOW))*.....28

FIGURE 5.2 FAULT 1 OVERVIEW ON THE LOCALITY 1 29

FIGURE 5.3 MEASUREMENTS ON THE CLIFF SECTION -LOCALITY 1 32

FIGURE 5.4 NORMAL FAULTS F1 AND F2A SEEN ON THE CLIFF SECTION......33

FIGURE 5.5 ZOOM ON THE NORMAL FAULT F4......34

FIGURE 5.6 A) LOCALITY 1 CLIFF SECTION AND BEACH EXPOSURE- F1 &F2AND B) EXAMINATION IN THE STRIKE, DIP AND THICKNESS DIMENSION DUE TO THE PRESENCE OF A CAVE AND IN THE LOWER PART OF THE HANGING WALL GOOD EXPOSURE THE FAULT CORE SEGMENTED.....36

FIGURE 5.7 LOCALITY 2-A) FAULT INTERPRETATIONS ON THE BEACH MNF (F5) AND OTHERS FAULTS, B) THE SYNCLINE 1 SEEN FROM THE CLIFF, C) NORMAL FAULTS RELATED TO THE MNF (F5)......38

FIGURE 5.8 OVERVIEW BETWEEN F7 & F8 INTERPRETATION ON THE CLIFF.....40

FIGURE 5.9 *OVERVIEW BETWEEN F12 INTERPRETATION ON THE CLIFF*.....41

FIGURE 5.10 RELAY RAMP SEEN IN THE LOCALITY 3 AND DIAGRAM TAKEN IN ACCOUNT IN THE INTERPRETATION......44

FIGURE 5.11 TO 1.3 KM EAST TO KILVE PILL, DIRECTION LILSTOCK, DOMES STRUCTURES AND AMMONITES......45

FIGURE 5.13 LOCALITY 3: FAULTS INTERPRETATION ON THE BEACH AND CLIFF SECTION; ONLY 3 FAULTS WERE INTEGRATED IN THE 3D GEOLOGICAL MODEL.(F13, F14 AND F15)......47

FIGURE 6.1 GEOREFRENCING PROCESS OVERVIEW......49

FIGURE 6.2 OVERVIEW THE GEO-REFERENCING INTO PETREL.....50

FIGURE 6.3 SCHEME SHOWING THE INPUT DATA FILTERED IN ORDER TO GENERATED THE HORIZONS AND FAULT SURFACE.....51

FIGURE 6.4 MAPPING WORKFLOW USED.....52

FIGURE 6.5 PETREL OVERVIEW OF THE LAYER AND FAULT SURFACE PROCEDURE.....53

FIGURE 6.6 MAKE SURFACE PROCESS.....54

FIGURE 6.7 OVERVIEW ISOCHORS SURFACES PROCESS BY BLOCK.....55

FIGURE 6.8 FAULT MODELLING PROCESS.....56

FIGURE 6.7 FAULT MODELLING PROCESS: FAULTS (SURFACES AND PILLARS), CONNECTION AND CONSISTENCY BETWEEN THEM.....57

FIGURE 6.10 PILLAR GRIDDING PROCESS.....58

FIGURE 6.11 PILLAR GRIDDING PROCESS: SKELETON GRID GENERATION BASE ON THE KEY PILLAR DEFINED IN THE PREVIOUS PROCESS. 59

FIGURE 6.12 FAULT INTERPRETATIONS: GOOD COMPARISON BETWEEN FIELDWORK AND PETREL. (CHECKING THE GOD MATCHING) 60

FIGURE 6.13 MAKE HORIZON PROCESS 61

FIGURE 6.14 MAKE HORIZONS PROCESS INCLUDES INTERPRETED HORIZONS AND QC IN THE STRATIGRAPHY SHOW IN 3D BY INTERSECTION (GRID I-DIRECTION). 62

FIGURE 6.15 MAKE HORIZON PROCESS: OVERVIEW OF SEGMENTATION (DONE BY BLOCKS). 63

FIGURE 6.16MAKE ZONES PROCESS SHOWING FROM TOP-L8 AND TOP-L19 INSERTED GEOLOGICAL ZONES IN THE STRATIGRAPHIC INTERVALS. 66

FIGURE 6.17 PROPERTY MODELING SCHEME 67

TABLE 6.1 *VARIOGRAM SETTING FOR THE SAND FACIES.* 68

FIGURE 6.18 QC THE FACIES MODELS GENERATED..... 68

FIGURE 6.19 GEOMETRICAL MODELLING SHOWING IN 3D VIEW: CONNECTED VOLUME AND FACIES PROPERTY GENERATED..... 70

FIGURE 6.20 PETROPHYSICAL AND FLUID PROPERTIES 71

FIGURE 6.21VOLUME RESULTS 72

INDEX OF TABLES

TABLE 2.1 DISCRETE PHASES _____ 15

TABLE 5.1 *COMPARISON OF THE DIPS OF THE SOUTH-DIPPING AND NORTH-DIPPING NORMAL AND REVERSE FAULTS* _____ 39

TABLE 6.1 *VARIOGRAM SETTING FOR THE SAND FACIES.* _____ 68

TABLE 11.1 *GPS POINTS COLLECTED IN THE AREA ACCORDING TO THE FAULT BLOCK* _____ 83

TABLE 11.2 *DIP AND STRIKE VALUES TAKEN IN THE CLIFF SECTION* _____ 84

Acknowledgments

This project of the Master Thesis has been performed with the Department of Petroleum Engineering, University of Stavanger (UiS), Norway, in cooperation with Total E&P Norge AS during fall term 2012.

It was supervised by Dr. Christopher Townsend whom I would like to convey sincere Thanks for his supervise and support on this project, adding enjoyable discussions on the field and useful tips regarding Petrel Software that served in enriching my knowledge.

I am really grateful with the Department of Petroleum Engineering, University of Stavanger for giving me the financial support on the field trip that was the occasion of fruitful exchanges between the field experience in addition with the interpretation of the structures seen and finally to build a proper 3D model of the area in study of my master thesis.

A Special Thanks to Lisa Bingham for her assistance in ArcGis tool and to Dr Alejandro Escalona for giving the opportunity be part/student of the Petroleum Geosciences specialization and provide to me the solid knowledge in sedimentation and key ideas in subsurface interpretation.

I would like to thanks to my husband, Freddy Oliveira for his patience, support, useful suggestions and critical remarks through the text. In Addition, I am very grateful with my God, family and friends who with enthusiasm and continue support helped me developing my thesis project.

1 Introduction

The trapping, the hydrocarbons' migration, and the evolution of the basins come from the normal faults systems. Recent works (*Walsh et al; 1991*) have demonstrated the evolution and geometries in well exposed areas, which provide a guide for the interpretation of the larger fault zones, as well as understanding the formation of oil and gas fields.

In addition to describing fault style and fault mechanism, much has been published in recent literature about the applicability technique to extensional basins. (Freeman et al, 1990)

The Faults and horizons geometries have been mapped from Lower Jurassic sequences on the cliff sections, and a well exposed wave-cut platform on Kilve Beach which lies on the south side of the Bristol Channel, England; UK.

The Kilve Beach area has been interpreted as normal fault system; their geometry and evolution play an important role for hydrocarbon reservoirs because oil and/or gas are frequently trapped in normal fault systems. Detailed studies of faulted outcrops help the understanding and interpretation of seismic data as they provide real geometrical examples to hang interpretations on. Additionally, they contribute in the understanding of how geological structures trap oil and gas. The Kilve Beach area was the influenced by faults and linkage between each other.

Strike and dip measurements were taken on the fault surfaces and limentones beds, adding to the last ones, thickness measurements. The beds correlations were generated according to the stratigraphic column in the cliff section generated by Brodahl, E. (1993), and for the tidal exposure that mapped by Kelly et al., 1998. The area is still subject to multiple interpretations and studies due to the complexity in the structures present on the outcrops.

The field data have been used to construct a 3D structural-stratigraphic model (into a 3D geological reservoir model) using the Petrel 3D modeling software.

A difference between this study and the previous studies (e.g. Brodhal 1985 and Øyvin 1995) is that the field data collected from the outcrops was interpreted to support a 3D geological model building of the area.

The detailed level in 3D geological modeling was constrained by the input and process time of the data (representing the horizon and faults as they were seen on the field).

1.1 Study Area

This study is based on outcrops examples from Kilve Beach area, which are situated on the southern of Bristol Channel basin, England. The Bristol Channel Basin belongs to a series of Mesozoic extensional grabens between Wales and Somerset (*Lindanger, et al 2007**)***. This Area is localised about 2 km from the centre of Kilve's town (*Figure 1.1*). The study area is characterised by Normal Faulting with fold geometries. From previous work realised (***Brodahl, 1993***) the rocks exposed on the Tidal platform and in the cliffs belong to the Lower Liassic age (Lower Jurassic).

The Fault zones have been described in small-scale at Kilve going into Lower Jurassic Limestone and mudrocks age (the ***grid references ST314-144-145 and ST315-144-145 shown on the Ordnance survey-Quantock Hills and Bridgwater-1:25000 scale***) (*Figure 1.2).* These faults are well exposed on the Limestone bedding and related with the development of the Bristol Channel Basin during the Mesozoic (***Beach, 1989***). According to Beach (1989), one of the fault showes evidence of strike-slip or reverse-reactivation that occurred in the Bristol Channel during the Tertiary. As mentioned above, the beddings exposed in the beach consists of limestone benches, whereas on the cliffs, these are formed by organic-rich shale interbedded with argillaceous limestone. The area is dominated by E-W striking normal faults, and small reverse movements identified on the Fault planes. The dip dimensions have been taken on the field over the faults and beddings (in the cliffs and the beach surface respectively).

The Field interpretation was done based on the maps (from the ***Ordnance survey-Quantock Hills and Bridgwater maps -1:25000 scale***), Photographs (taken on the Field), satellite images (digitized from *Anquet map 2011*software in combination with those given by *Google earth*) GPS measurements points. The data and interpretation were used to build the 3D geological Model in Petrel.

These localities have been mentioned above by Elizabeth Brodahl in 1993, Steen Øyvind in 1995, and other researchers. The fieldwork was carried out in three locations (***location 1***-Kilve Pill, ***location 2***- starts in **F5** identified as major fault 1 (overview of syncline 1) - and ***location 3***- starts

in F13 (overview of syncline 2)-). This area represents approximately 1, 5 Km from Kilve Pill to the east part direction Lilstock, where the beach is facing towards the north. (*Figure 1.3*)

1.2 Objectives

The purpose of this study is to describe the behavior of the faults and horizons on the Kilve Beach outcrops (a faulted area with Liassic limestone and shale beds), in the Southwest of England by using field work data collection and the construction of 3D structural model of the area. (*Figure 1.4)*

The field work objectives included the mapping of the key horizons and structural elements (faults), using detailed stratigraphic correlation

The structures were mapped by making outcrops observations and the acquisition of relevant field data using GPS measurements, as well as air photos and satellite images.

Finally, a 3D model of the fault blocks interpreted was built by using *Petrel* ™ software. This model may be used as an analogue for oil and gas fields.

1.3 Previous works

Most of the references on this study come from previous data, taken in the Kilve Outcrops studies which are unpublished Msc theses (such as Brodahl, E. 1993 and Steen, Ø. 1995). These studies presented detailed stratigraphic correlations, and field observations using dip meter logs which were used to recognize in small and big scale, the main structures and major faults of the area.

Brodahl, E. (1993), mapped the structures location which extends around 6 km along the Kilve Beach. The cliff exposures projections were taken by measuring the length, displacements, thickness, lithology and the fault planes. She claimed that the Kilve location was dominated by a fractal extensional deformation where the main faults were normal faults, including the antithetic faults found in the East of Bristol Channel Basin. In addition, she documented a detailed profile of the cliff, and showed a map of stratigraphic framework of the sections helped with photographs, which were taken during the fieldwork in combination with the aerial photographs from the territory

Steen, Ø. (1995), tested the reliability of fault interpretations by studying the geometry of the faults and their associated fold outcrops of Kilve Beach. The deformation related to normal faults in Kilve include normal drags fold, reverse drag folds and roll-over anticlines above listric faults. Steen claimed that the width and accentuation of normal drags folds in Kilve tend to saturate for faults displacement from 10 m up to 60 m.

The tectonic influence on deposition and stratigraphy framework was described by *Tankard et. al (1989),*who included the Bristol Channel as part of Celtic Sea Basin and claimed that it had been subjected to three discrete phases of extension and fault controlled subsidence, each phase was followed by a period of thermally controlled passive subsidence. The outcrops studied belong to Lias, which has extensive subcrop in England. Their thick successions have been proven by boreholes in the North Sea, Hebrides Sea, Irish Sea, Bristol Channel and Cardigan Bay (*Simms et al., 2004*). Moreover, the Lower Lias stratigraphy was used from the Palmer's interpretation in 1972 and Whittaker and Green, (1983), followed in detail by Brodahl, E., (1993). That was treated in combination with Peacock's paper (1998) about the tectonic evolution of the Bristol Channel Basin, the linkage and interaction in normal fault systems, has been taken into account to understand the geometries and evolution of Normal Faults in the Jurassic sedimentary rocks of the Somerset coast.

A study from Peacock and Sanderson (1994) interpreted the relay ramp in the east of Kilve Pill. They described the relay ramp as open and continuous structure that maintains the continuity between the footwall and hanging wall. In suitable outcrops, fault tips involved in the relay ramp can be observed directly, whereas in seismic data there is an inherent resolution limit below which discrete fault geometries cannot be imaged (*Townsend et al., 1998*).

Conford (2003), interpreted the presence of domes structures to 1.3 km east to Kilve Pill in the direction Lilstock. The domes structures were uplifted in the carbonate and were prominent as a result of erosion overlying mudstones unit. In addition, these structures were shown in the hanging wall of the relay ramp interpreted by Peacock and Sanderson (1994).

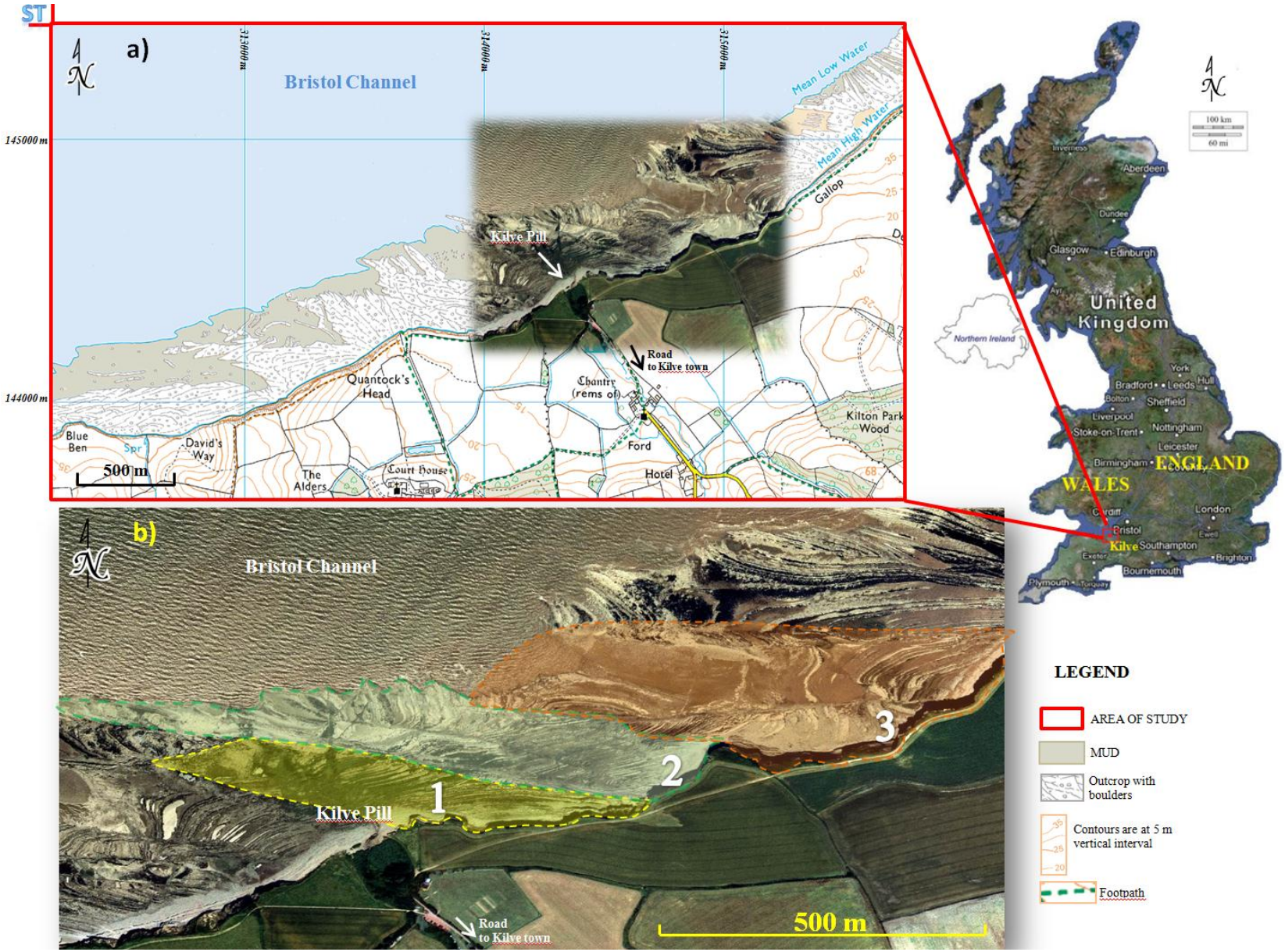

Figure 1.1 *Combination of Topographic Map of the Southwest of England and satellite image, showing the location of Kilve Beach and the three localities where the fieldwork was carried out. Based on a small part of Ordnance Survey from Anquet maps 2011, originally 1:25,000 scales.*

2 Geological Context

The study area is located in the Kilve Beach, southern margin of the eastern branch in the Bristol Channel Basin (*Figure 2.1 and 2.2*). It belongs to the Mesozoic Grabens in southern England (*Glen & Whittaker, 2005)* and Celtic Sea basins (*Figure 2.2).* The area is of a normal fault series outcrops. The basin has been subject to three discrete phases of extension and fault controlled subsidence which could be recognized, each phase was followed by a period of thermally controlled passive subsidence (*Tankard et. al 1989*) as shown below:

Table 2.1 *Discrete phases*

	Phase Extension	Passive Subsidence
1	Permian to Triassic (Synrift I)	Hettagian to Oxfordian
2	Late Jurassic (Synrift II)	Tithonian to Berriassian
3	Early Cretaceous (Synrift III)	Aptian to Maestrichtian

The first phase, Synrift (I) is a series of northeast-southwest trending controlled by small faults, and isolated basins probably developed in the Late Permian (*Van Hoorn 1987*). The facies development in the axis of Bristol Channel basin were dominated by evaporitic mudstones, grading upward into massive halite and later on, these mudstones grade upward into a restricted marine latest Triassic sequence of anhydritic mudstones, sandstones and limestones, reflecting the start of the major marine transgression.

The first passive subsidence was associated with a combination of local variations in subsidence rates, and more widespread changes in sea level (*Millson 1987*). The deposition during this period was characterized by a series of regressive-transgressive cycles, within a gently subsiding basin. It started in the Hettagian with an initial regression, followed quickly by a transgression in the Late Triassic, resulting in dominant mudstone facies and thin cycles of micritic limestone. Just before the Sinemurian, a basin wide transgression started characterized for open-marine

conditions where the sedimentation process was dominated by mudstone and thin limestones. The late Oxfordian was assigned as unconformity (*Millson 1987*).

The Synrift (II) was the result of the faults reactivation controlled by subsidence in the pre-existing Triassic rift basins, and initiation of further basins (*Masson and Miles 1986a*). The structural response, uplift and erosion were associated with an extensional episode where the Bristol Channel basin was actively subsiding. Fluvio-lacustrine and lagoonal to marginal-marine facies were developed.

In the second passive subsidence, it was active extension and fault controlled subsidence continued, which was associated with substantial uplift of the basins ended. The marine influence over the interbedded coarse clastic and limestone was developed (*Tankard et. al 1989*).

The Synrift (III) phase is a series of northeast-to-southwest and east-west trending extensional faults, which were reactivated in a translational sense in the Celtic Sea basins (*Van Hoorn 1987*). One of the Celtic Sea Basins, The Bristol Channel basin, was dominated by transgressions through the Early Cretaceous. The facies were developed in a marine transgression.

During the third passive subsidence, uplift resulted from local changes in subsidence rates and possible regional changes in sea level. Transgressive clastic facies units were developed (*Tankard et. al 1989*).

The local structural Framework was given by extensional faults behavior, exposed on the outcrops. These outcrops belong to the Lower Jurassic series in Britain, and unbroken strips of different thickness, extending from East Devon and West Dorset Coast, north-northeast through Somerset, Gloucestershire, the east Midlands and Humberside, in the coast of Cleveland and North Yorkshire (*Simms et al., 2004*).

The Eastern of the Kilve Area (locality 3, *Figure 4.XX*) is characterised of the Early Lias formations (started in the Triassic) with several metres of beds above the Penarth Group, and identified as younger formation. From here it runs through the Hettangian Stage of the Lower Jurassic, and into the Semicostatum Zone of the Sinemurian Stage, where the cycles of limestone and shale gradually change into the predominantly mudstone. In addition, a variety of fossils

record is preserved on beds in the Kilve area. Additionally, the large ammonites were found in the area, which is visited by several research groups due to the fantastic exposures and easy access to the beach.

2.1 Outcrop Structural Review

The outcrops studied belong to the Lias, which has extensive sub-crop in England (*Figure 2.2).* A series of investigation of both onshore and offshore outcrops/sub-crop by drilling and geophysical methods, in association with hydrocarbon exploration, has revealed the nature, extent and structure of Lower Jurassic in Britain. Their thick successions have been proven by boreholes in the North Sea, Hebrides Sea, Irish Sea, Bristol Channel and Cardigan Bay (*Simms et al., 2004*).

2.2 Outcrop Stratigraphy Review

The lower Jurassic rocks of Great Britain are predominantly marine mudstones that have been grouped together under the name "Lias" since the early part of the 19th century. They form a distinctive succession of marine carbonates where the Lias was deposited in a series of interconnected sedimentary basins and shelf areas, producing local differences in the sedimentary successions (*Simms et al., 2004*). Nonetheless the local successions were correlated, and some stratigraphic levels have been recognized across the largest outcrops studied in Kilve Beach.

Stratigraphic framework of the Lower Lias for the cliff section used in this study was mapped by Brodahl, E. (1993) (the measurements were taken in 109 beds in the cliff at the west of Lilstock and 39 beds on the foreshore east of Kilve) , following the Palmer (1972) and interpretation and Whittaker and Green, (1983), where the sequences were correlated to the biostratigraphy; combining with that mapped by Kelly et al, (1998) on the foreshore taking in account the stratigraphy generated by Whittaker and Green, (1983) in order to generate a good correlation between outcrops. In addition, the resolution of the images allowed accurate placement of the stratigraphic boundaries. (*Figure 2.1).*

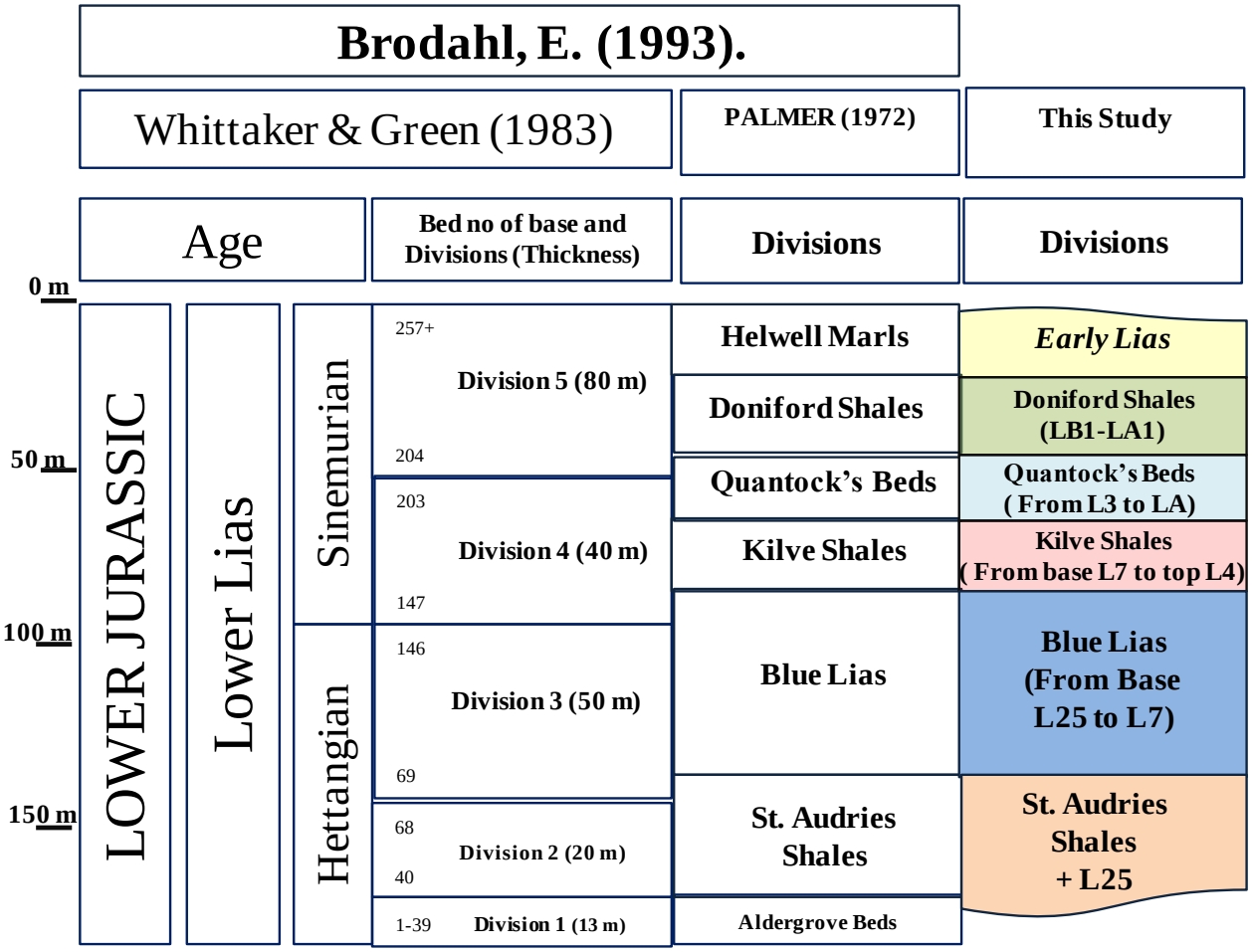

Figure 2.1 *Stratigraphic correlation of the Lower Liassic exposure at Kilve Beach, compared to published accounts (modified by Brodahl, E. (1993) and Kelly et al, 1998)*

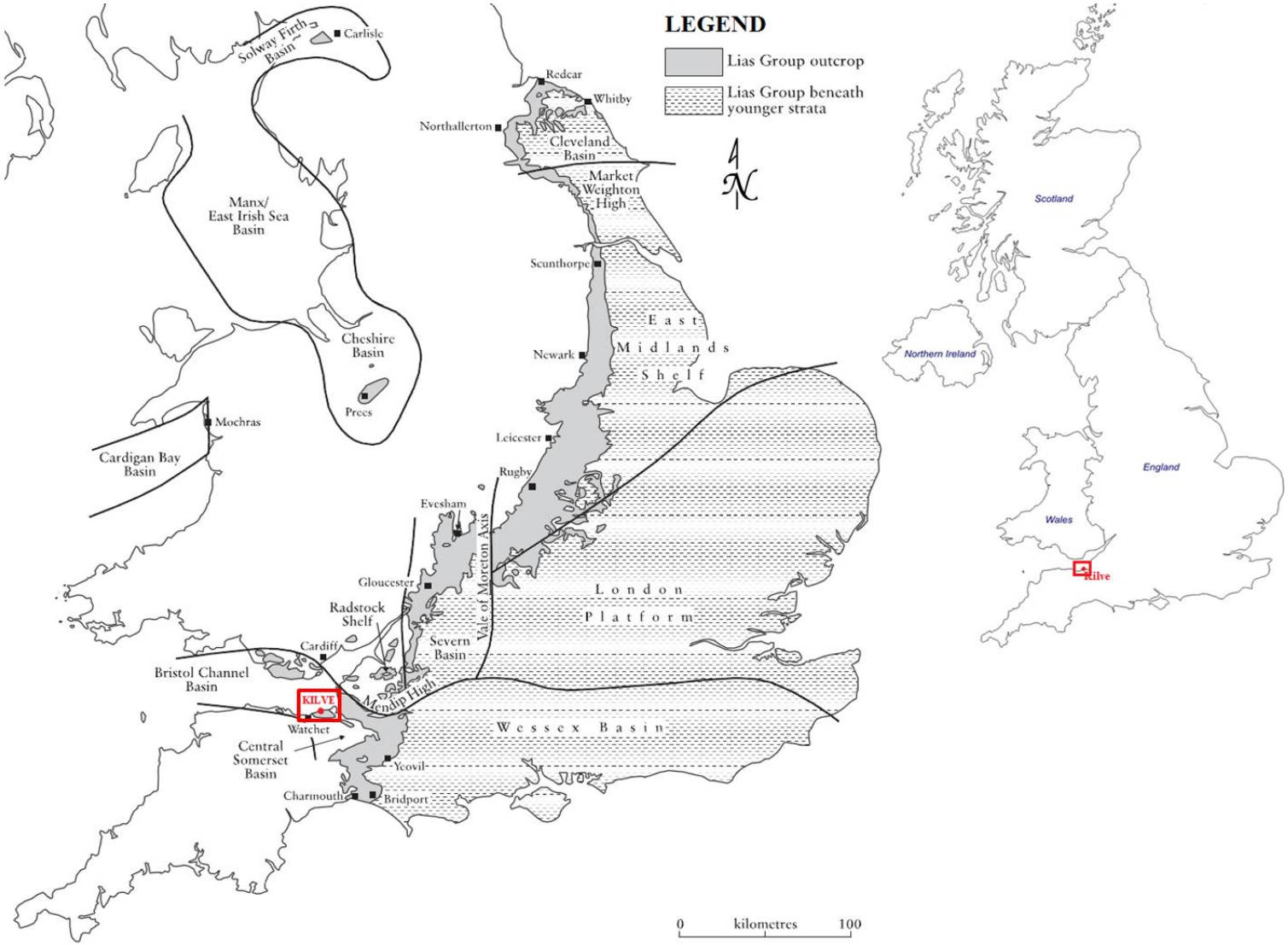

Figure 2.2 *Outcrop and subcrop Lias Group in England and Wales showing the Kilve location and main sedimentary basin. After Cox et al. (1999) and Simms et al.(2004)*

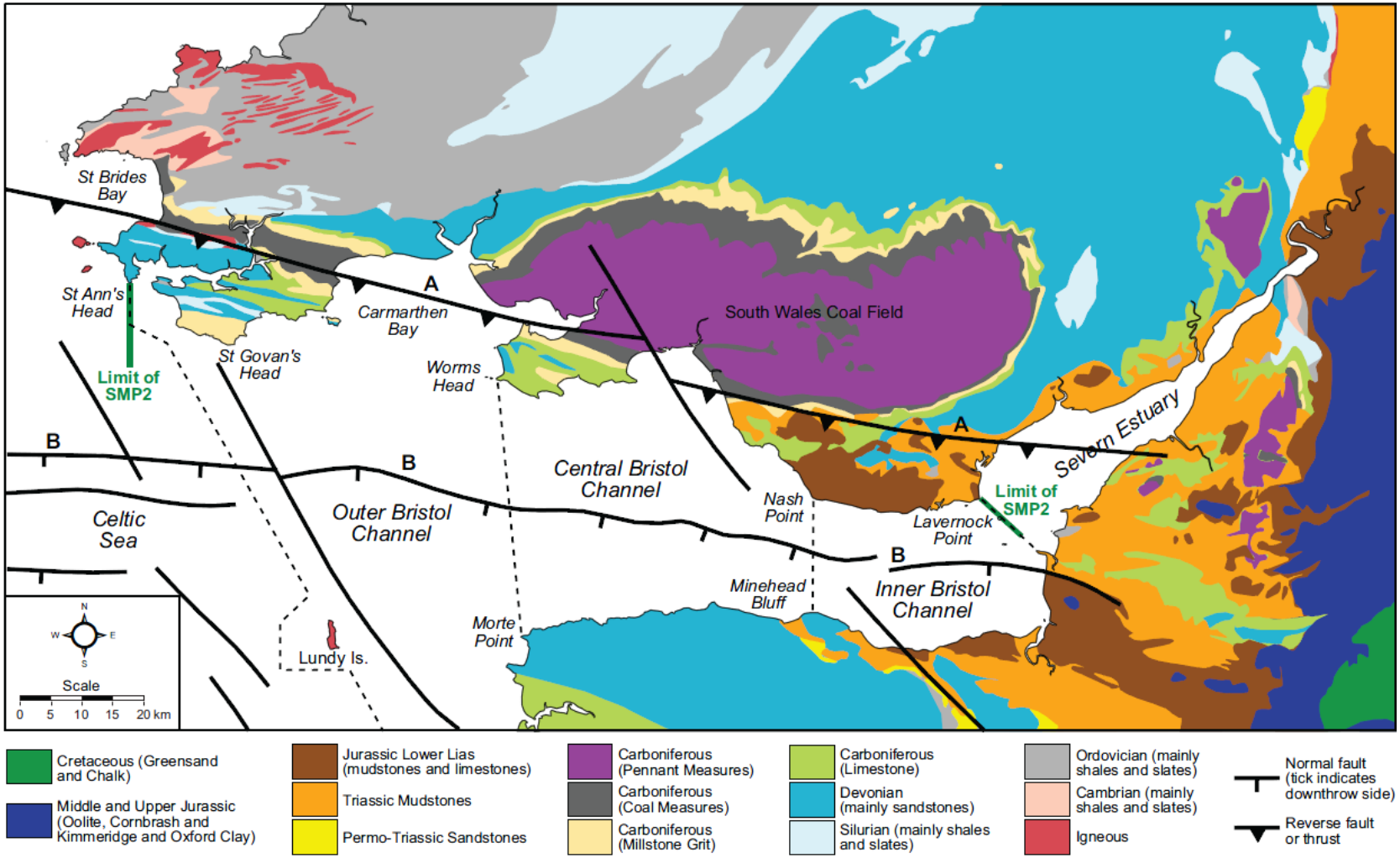

Figure 2.3 *Major geological features of South Wales and the Bristol Channel based on British Geological Survey maps and Tappin et al. (1994). A = Variscan Front Thrust, B = Central Bristol Channel Fault Zone.*

3 Fault Description: Theory review

For the geoscientist, it is important to get an overview about the structural geology concerning the faults analysis. A fault can be transmitter or barrier to fluid flow and pressure communication. The understanding of the fault behavior is fundamental for hydrocarbon fields drilling, exploration and development.

According to the data collected in the field, analysing the major structures (dominated by normal faulting), and recent works developed in Kilve Beach area, the area is presented as an extensional settings. The small reverse faults interpreted on the outcrops will be shown as overview but not described in detail.

Key definitions and drawings are shown in order to explain different components that should be taken in account in fault analysis.

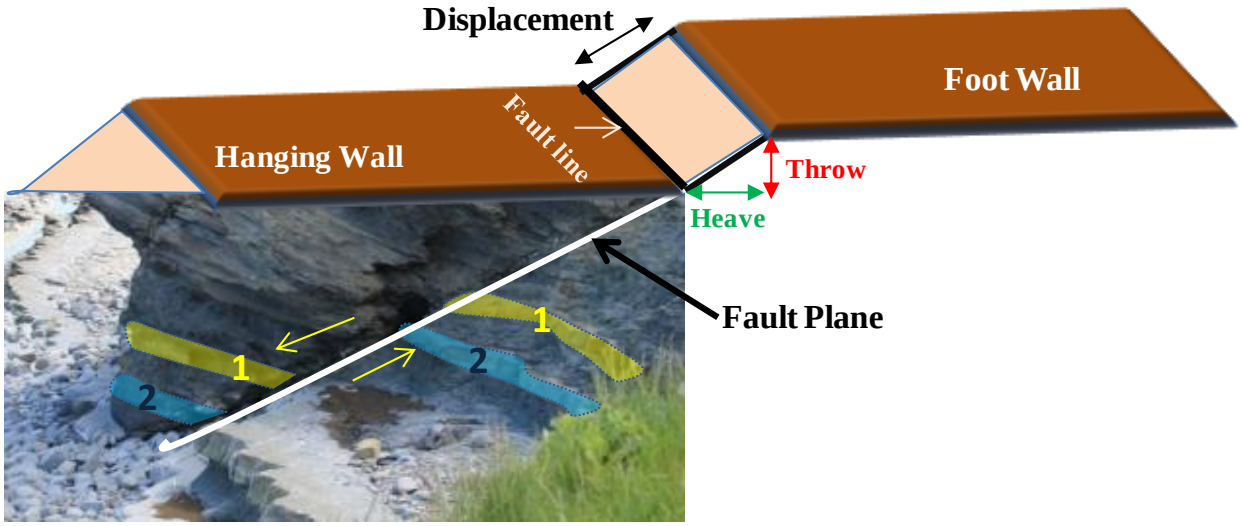

Figure 3.1 *Example of Normal fault with its dimensions*

Fault zone: a zone containing a number of sub-parallel or anastomosing fault surfaces.

Fault: a surface along which appreciable displacement has taken place; this surface may be planar or curviplanar (listric).

Footwall: the body of rock immediately below a non-vertical fault. The body of rock itself is called the footwall block.

Hanging wall:the body of rock immediately above a non-vertical fault. The body of rock itself is called the hanging wall block.

Throw: vertical component of fault displacement.

Heave: horizontal component of fault displacement.

Fault displacement: The offset of segments or points those were once continuous or adjacent. Rocks beds that have been moved by the action of faults showing displacement on either side of fault surface.

Extensional Fault: a fault which produces horizontal lengthening as measured across the trace of the fault.

In the study area, it was identified two major structures and minor structures associated which help in the evolution of the normal faulting. These played an important role in the faults correlation minimizing the risk in the regional context. *Figure 3.2* shows these structures on the cliff.

Major Structure: is the largest observed size (fault with most important throw, largest structure)

Minor structure: is the lower size compared to major one and/or which development is directly related to the major structure.

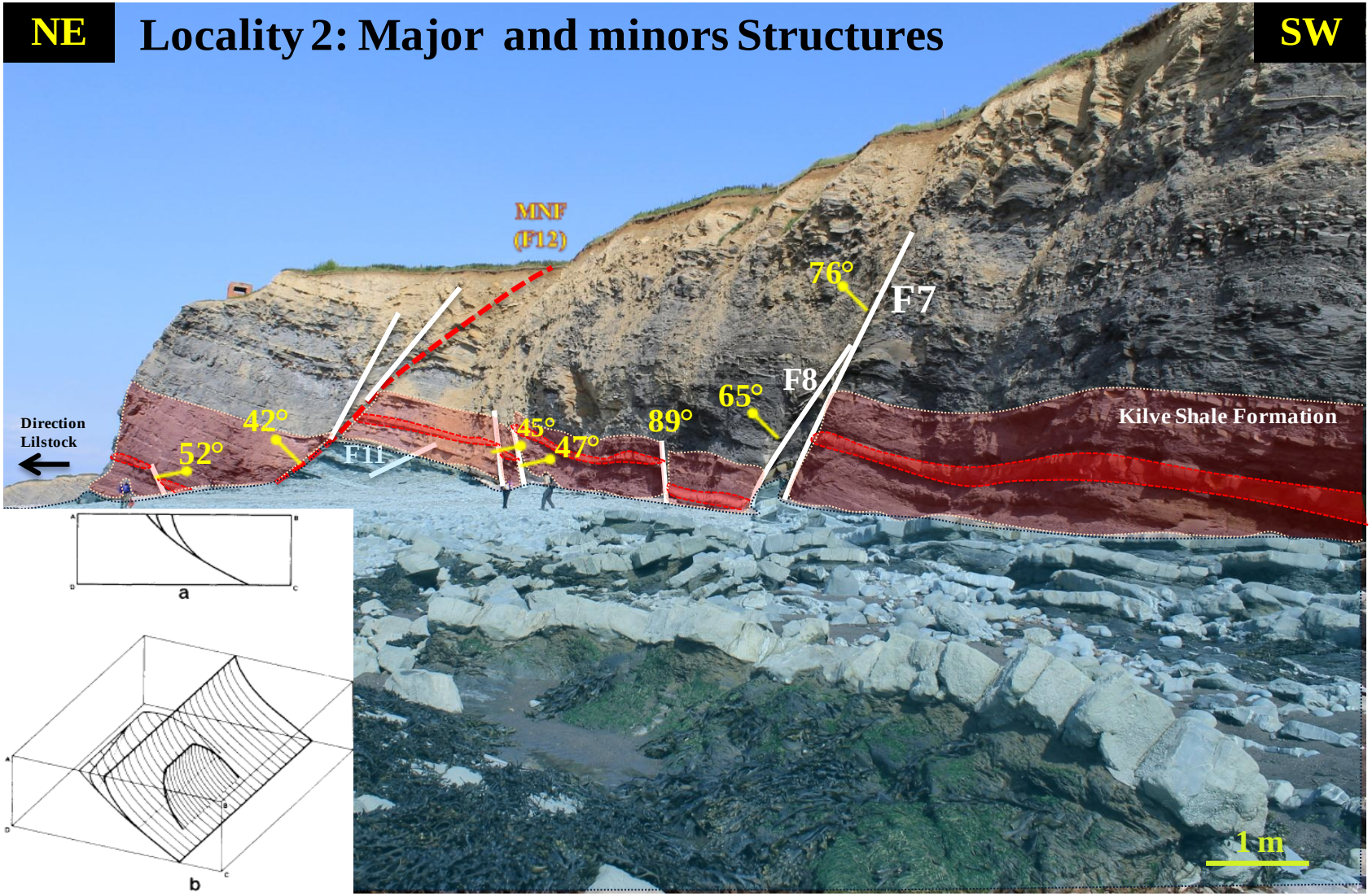

a) Cross section of a fault with 2-hard linked splays as show in the Major Normal Fault-F12 and b) Block diagram showing the geometry in 3D

Figure 3.2 *Field example showing mayor and minor structures.*

4 Measurements and Notation

- The devices used consist of a ruler, measuring tape (10 m), GPS (Garmin-using Waypoints indicating the latitude and longitude coordinates even in degree or cardinal letters (N,S,E,W), the accuracy of this device is <10 m (33 feet) 95% typically), Compass Burton and Camera (with a small tripod).
- Fault displacements were measured using the ruler and the measuring tape (the errors are subject to the irregular nature of the bedding planes)
- The faults interpretation and mapping were produced using photographs taken in situ and maps from Anquet maps (a program commercially available on the Ordenance Survey in UK) helped with the Google Earth photos as base maps. In order to have good resolution and vision in different angles of the land exposures, the photos were taken from the top of cliffs to visualize the tidal platform and around 5m from the beach exposure to show the cliff sections.
- On the faults, it was measured the strike-dip (using compass brunton), the limestone bedding planes related to these with the bed height measurement respectively.

A&B) strike /Dip measurements and interpretation according to the bed plane

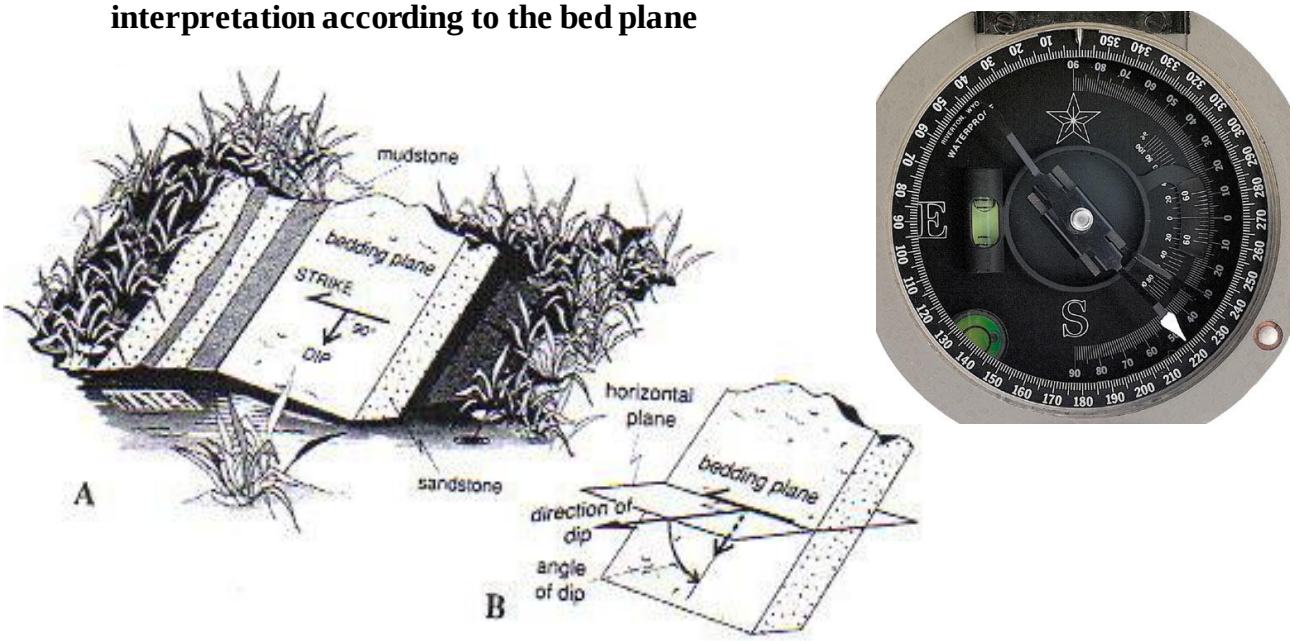

C. – Acquisition of GPS points and D.- Measuring tape of 10 m.

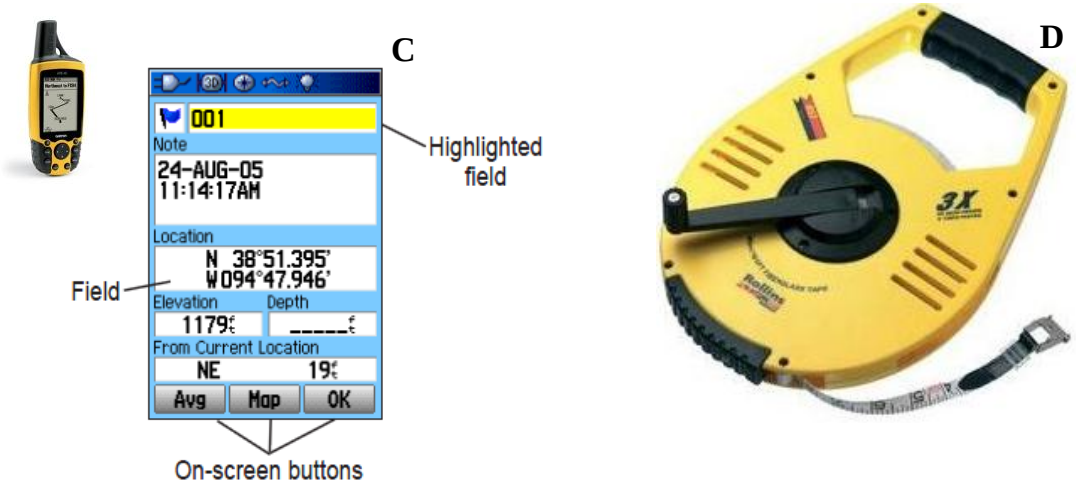

Figure 4.1 *Tools used in the measurements and notation*

5 Data Collection and field Observations

The fault zones (to be described later on this report), are located on the Onshore-Lower Jurassic limestone and shale at Kilve Beach in Bristol Channel, South of England. The faults were well exposed on the cliffs (up to 40 m high) and on the tidal flat (up to 500 meter wide) *(Øyvind, 1995).*

The Kilve Beach is facing towards the north and the E-W oriented Bristol Channel Basin. The area is dominated by normal faults probably related to a series of events occurred in the Bristol Channel basin during the late Jurassic- Early Cretaceous.

5.1 Outcrop data

The layers' surfaces on Kilve Beach outcrops were continue on the cliff, and around 80%-90% of exposure on the beach, most of them were parallel to each other (sandstone-shale-sandstone) and very distinctive. The sandstone surfaces were easy to recognize and be followed across the outcrops and faults.

The thicknesses were measured using measuring tape. For those cases where the thickness was not exposed, the strike and dip values were estimated. The length of some faults accessible, and well exposed were also measured. The dip and strike measurements were taken with a compass on the beddings and fault surfaces.

The major sedimentary and structural elements in the outcrop were identified. All faults and beddings were mapped at a scale of 1:25000, both in plane and profile/cross-section. These beddings were inside an extensional system composed by several normal faults where 14 of them were identified as normal where 2 were selected as major normal faults due to the length dimension and several branches (both identified on the locality 2) and 4 small reverse (*Figure 5.1).* These were also named as MNF1 (F5 in *Figure 5.8*) is related to the Syncline 1 and MNF2 (F12 in *Figure 5.9*) respectively.

The exposure of the normal faults interpreted in the cliff section and Beach platform are mainly striking E-W (from 5° to 358°)**.** It was observed 3D geometries insight of some of the faults. In general, the faults were dipping toward the north (i.e. face to the basin) with few of them dipping to the south and often steeper. The beddings were dipping toward to the south, although locally these deviates due to folding related to the faulting.

The outcrops were photographed in direction E-W (general striking) *Figure 5.1*, it was used as data base and due to the high resolution of the images, the interpretation was done fast while giving guidelines to improve the interpretation of the structures.

The Data collected of the beddings and faults structures was supported by:

- Visualization of the area by maps, air photos from Anquet, adding the google earth and photographs.
- Front to the cliff section, a visual scan around 5 m was done in combination with photographs and satellite images in order to describe and recognize the orientation (strike/slip) of the beddings and faults. Also, other structures were analyzed such as: spacing, high of the bedding, measurements on the fault lengths (in the zone of easy access) and displacement.
- The bedding and faults were named in combination with strike and dip measurements, helped the correlation of the beddings (between cliff and beach section) by looking for their relationship and orientation.
- Into the 3D modeling, the fault interpreted helped to determine the beach structures by blocks or segments.

The maps (from Ordnance survey inside Anquet maps) in combination with the points measured from GPS and data taken on the outcrops faces allowed to build a 3D model into Petrel.

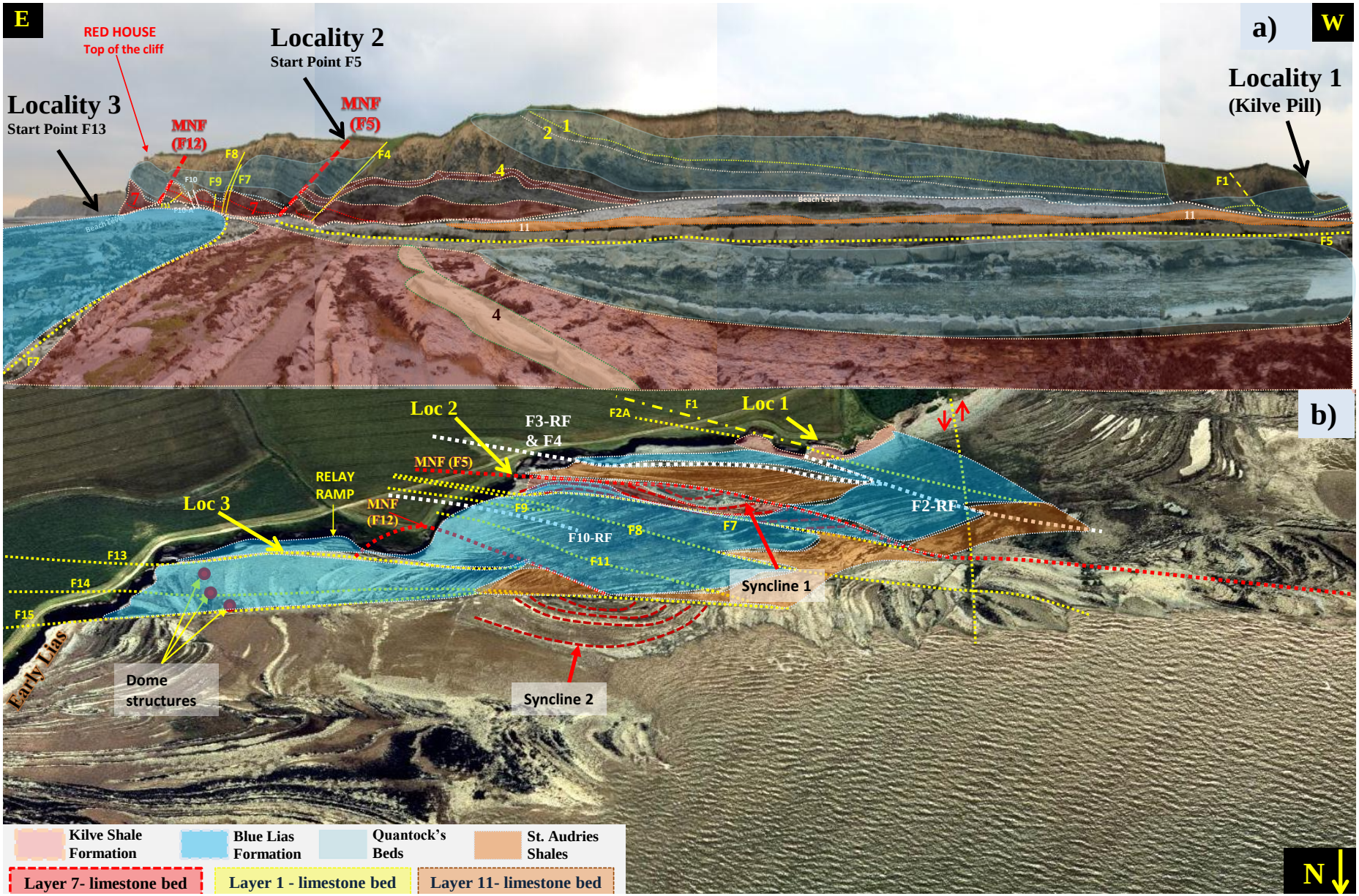

Figure 5.1 a) *Profile on the Cliff and b) the Beach exposure, Faults interpreted (2 major Faults (in red), into the minors faults are 2-reverse faults (in white) and 9 normal faults (in yellow))*

5.1.1 Locality 1 (Kilve Pill)

It is the coastal path along the northern flanks of the Quantock hills. This section is characterised by an excellent outcrop exposed on the cliff (*Figure 5.2)*, which is pointing to the North showing a normal fault (Identified as the Major fault) where the bedding/rocks above the fault surface have slipped down-wards and the limestone bands in the cliff foot have been faulted down about 3, 5 m, below the beach level in the block forming the head land. The fault is striking N15°W presenting a dip of 45° towards to the North.

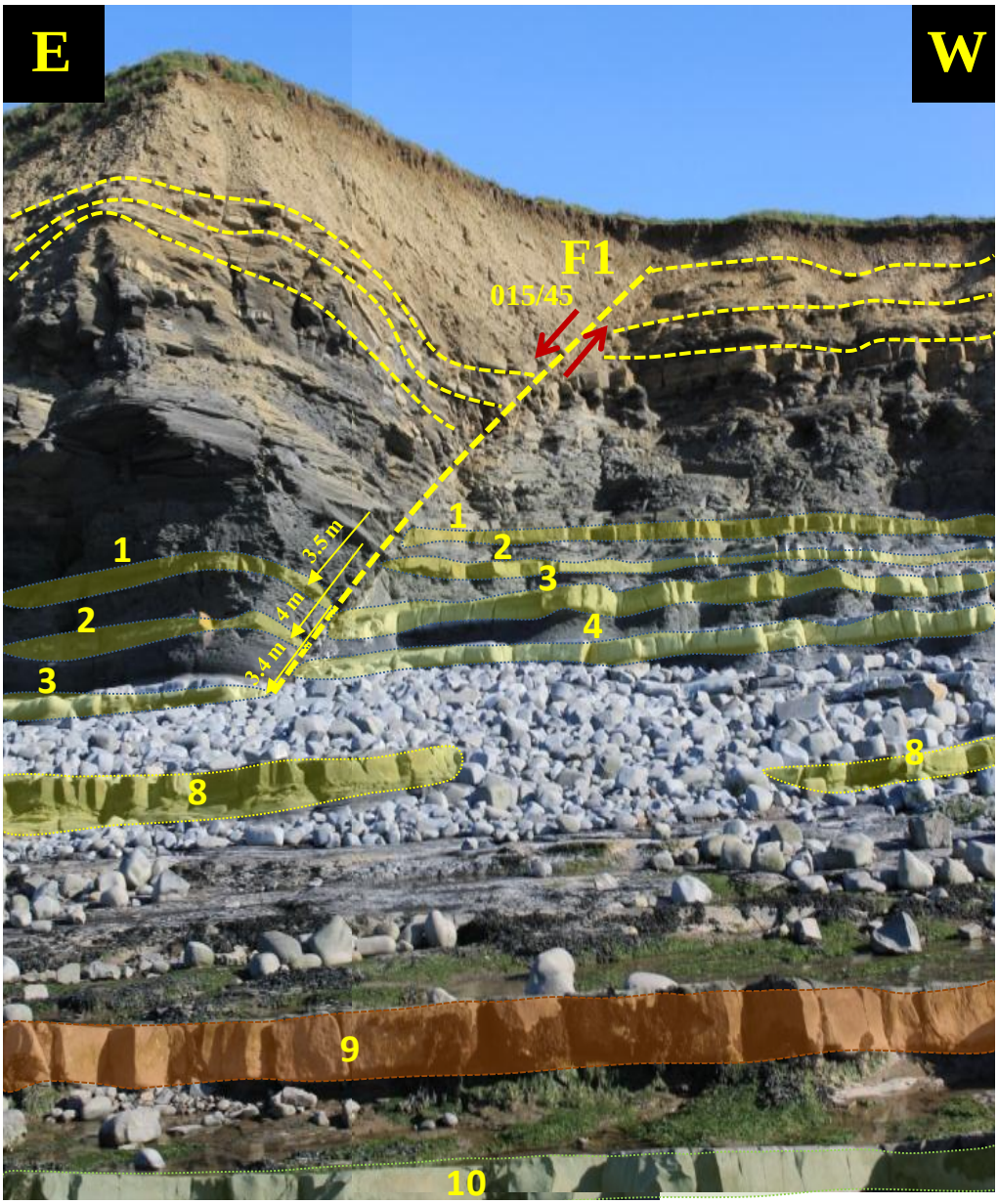

Figure 5.2 *Fault 1 overview on the locality 1*

5.1.1.1 Locality 1 Layers Description

On the first Cliff section, six layer (limestone beds) were identified as oldest deposition, from layer 6 on the base of the cliff and layer A on the top of the cliff following the stratigraphic sequences generated by Brodahl, E. (1993) and the author interpretations (*Figure 5.3*). The youngest ones in place are in the eastern part of the area, near to the last study location (*locality 3)*. (*Figure 5.4)*

The limestone beds shows on the cliff have been correlated across the faults (F1 and F2 defined as the big ones). Some Normal drags structures on the footwall and hanging wall shown that effectively it was a normal fault. Towards the eastern of the cliff, there are indicators of small reverse movements (*Figure 5.4)*. But these are not shown in the west side of the cliff studied on this location 1. In general, the rocks associated to the fault and interbedded shale with limestone benches.

On the cliff section, the thickness of limestone beds in the hanging wall varies between 15 cm and 35cm while in the footwall varies between 22 cm to 44 cm, for the shale beds it could vary between 43 cm to 1.2 m (*Figure 5.5*). The dipping of these layers is towards to the south-west with an average of 19° in the footwall and 13° in the hanging wall .

The fault (F1) damage zone was around 80 cm thick in the footwall and 1.2 m in the hanging wall observed as small tension fractures varying in orientation east-west most of them without any measurement in displacement. In the fault plane was observed a thin fault core with a small thickness around 6 cm in the upper part (up the limestone layer 1) and the lower part (near to the beach level) and around 60 cm in the middle part (close to the limestone layer 1 and 2); in addition, the fault core consists of predominant limestone and the thickest shale fabric parallel to the fault surface.

On the beach, there was a well exposure of which block is the footwall and hanging wall, also a good orientation of the fault surface and beds which basically present the same type of rock shown on the cliff. (*Figure 5.6, 5.5 and 5.6)*

On the beach exposures, the thickness of limestone beds (marked as numbers on the section) in the footwall are between 14 cm to 50 cm, in the hanging wall varies between 20 cm and 40 cm, and for the shale beds it could vary between 17 cm to 3 m. The dipping of these layers are

towards to the south-west with an average of 13° in the footwall and 10° in the hanging wall, also no significant rotation anticlockwise during the faulting. (*Figure 5.5)*

After the second fault (F2A) seen in the cliff, a long cliff section with parallel layers were observed where three thick limestone layers were identified close to the beach level separating with a massive mud rock around 2 m the youngest layers (identified as A,B and C respectively) and later on those disappear. (*Figure 5.1)*

On the beach section a third fault was interpreted named F3, start in the layer 6 and die out on the fault F2, the layers are also parallel showing a dip average of 10 ° toward to the south and N84W then it was linked with the F4 and the end of the long cliff section. (*Figure 5.4)*

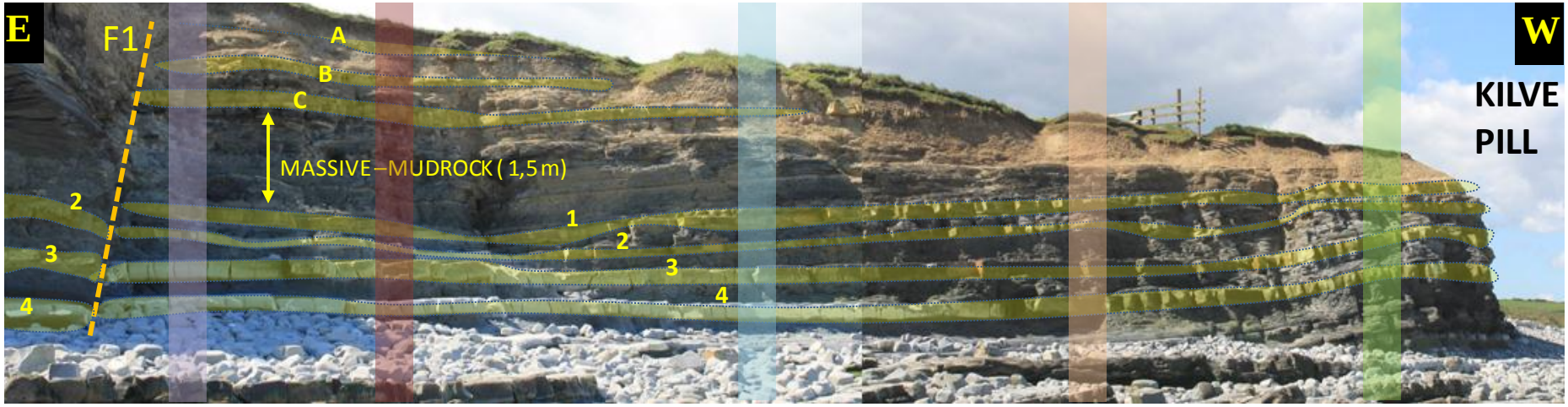

				Azimut Notation		Quadrant Notation							
Line	*Layer*	*Distance (z) cm*	*between (Sh) cm*	***Strike***	*or*	*Direction from*	*Angle*	*Direction to*	*Direction from*	*Angle*	*Direction to*	***Dip***	*Direction*
A	1	29	43										
	2	23	1,1	165	345	S	15	E	N	15	W	15	SW
	3	36	90	154	334	S	26	E	N	26	W	12	SW
	4	35	1,2										
B	1	25	52	150	330	S	30	E	N	30	W	14	SW
	2	23	1,15	166	346	S	14	E	N	14	W	10	SW
	3	44	93	170	350	S	10	E	N	10	W	12	S
	4	37	1,1										
C	1	27	55	155		N		S					
	2	23	1,15	155		N		S					
	3	41	80	155	335	S	25	E	N	25	W	11	S
	4	38	93										
D	1	25	50	166	346	S	14	E	N	14	W	14	SW
	2	23	90	150	330	S	30	E	N	30	W	15	SW
	3	44	65	145	325	S	35	E	N	35	W	7	SW
	4	35											
E	1	26	45	157	337	S	23	E	N	23	W	13	SW
	2	22	75	151	331	S	29	E	N	29	W	5	SW
	3	42	62	158	338	S	22	E	N	22	W	13	SW
	4	35											

Figure 5.3 *Measurements on the cliff section -Locality 1*

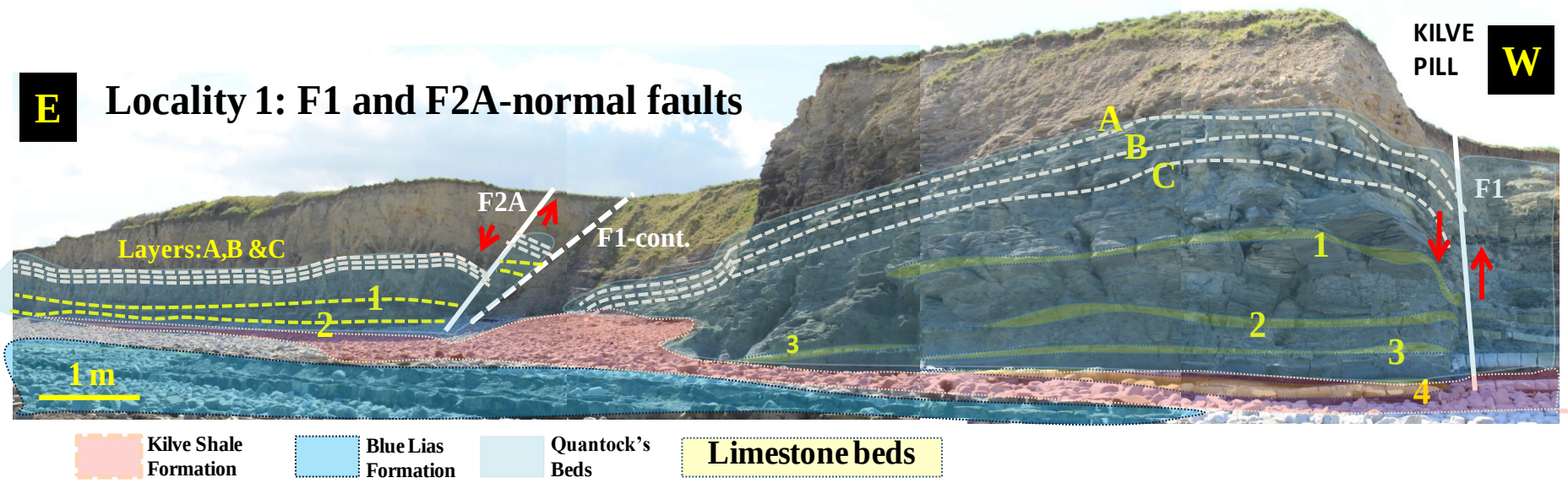

Figure 5.4 *Normal faults F1 and F2A seen on the cliff section.*

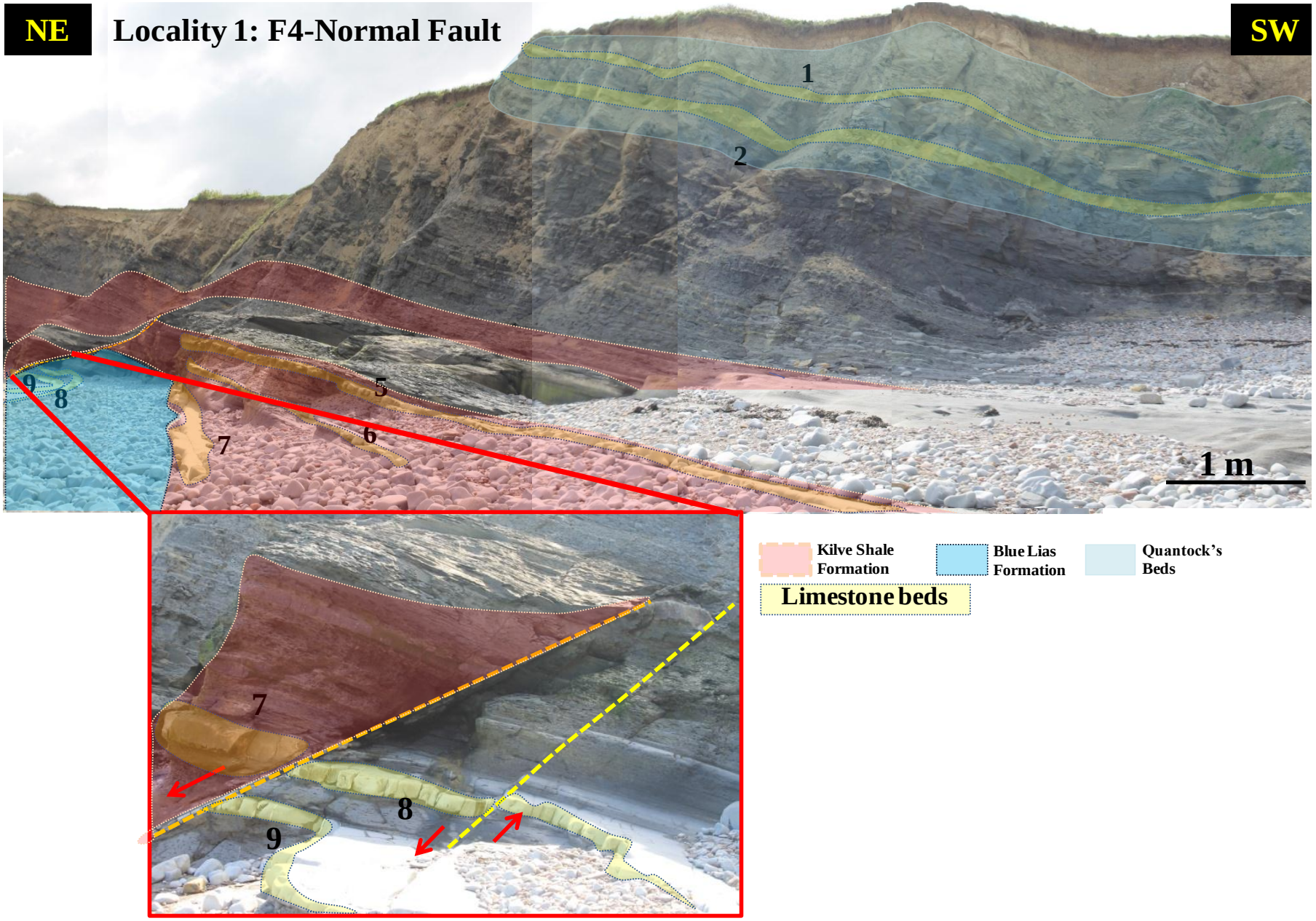

Figure 5.5 *Zoom on the normal fault F4.*

5.1.1.2 Locality 1 Faults Description

The geometries of the faults can control whether a fault zone act as a fluid conduit or barrier (e.g. Caine et al. 1996).

Five faults have been identified on the location. Three normal faults were interpreted on the cliff section (as normal F1-F2A and F4) and two on the tidal exposure (as reverse F2-F3) probably linked to the reverse movements caused by the faulting. The faults interpreted were orientated towards the north.

Through the fault surface (F1) on the hanging wall the strike and dip dimension of one layer could be measured due to the presence of a cave close to two limestone layers (named 1 and 2). (*Figure 5.1.3*).The outcrop is sub vertical where the fault displacement shows along a 10, 2 m high and 12 m long section. (*Figure 5.1.1*)

On the eastern part of the cliff close to Kilve Pill, the first normal fault (F1) was continued presenting a different dip measurement 48° also toward the north. A second fault (F2A) was interpreted close to the F1-continuation, in the field, the F2A and F2 (seen in the beach exposure) could be interpreted as the same fault, but it was not the case, because the F2A was a normal fault presenting 58° of dip and N20W striking while that exposed in the beach F2 was interpreted as small reverse fault according to the layers displacement presenting 61° of dip and N10W striking.

After the second normal fault (F2A), long section cliff shown good exposure of parallel layers (*Figure 5.4*), the dip of the layers presented an average of 11° toward to the south and N75W striking. A third fault was interpreted as reverse on the beach section, named F3, not seen in the cliff and dies out on the F2 with 52° of dip toward to the north and N25W striking.

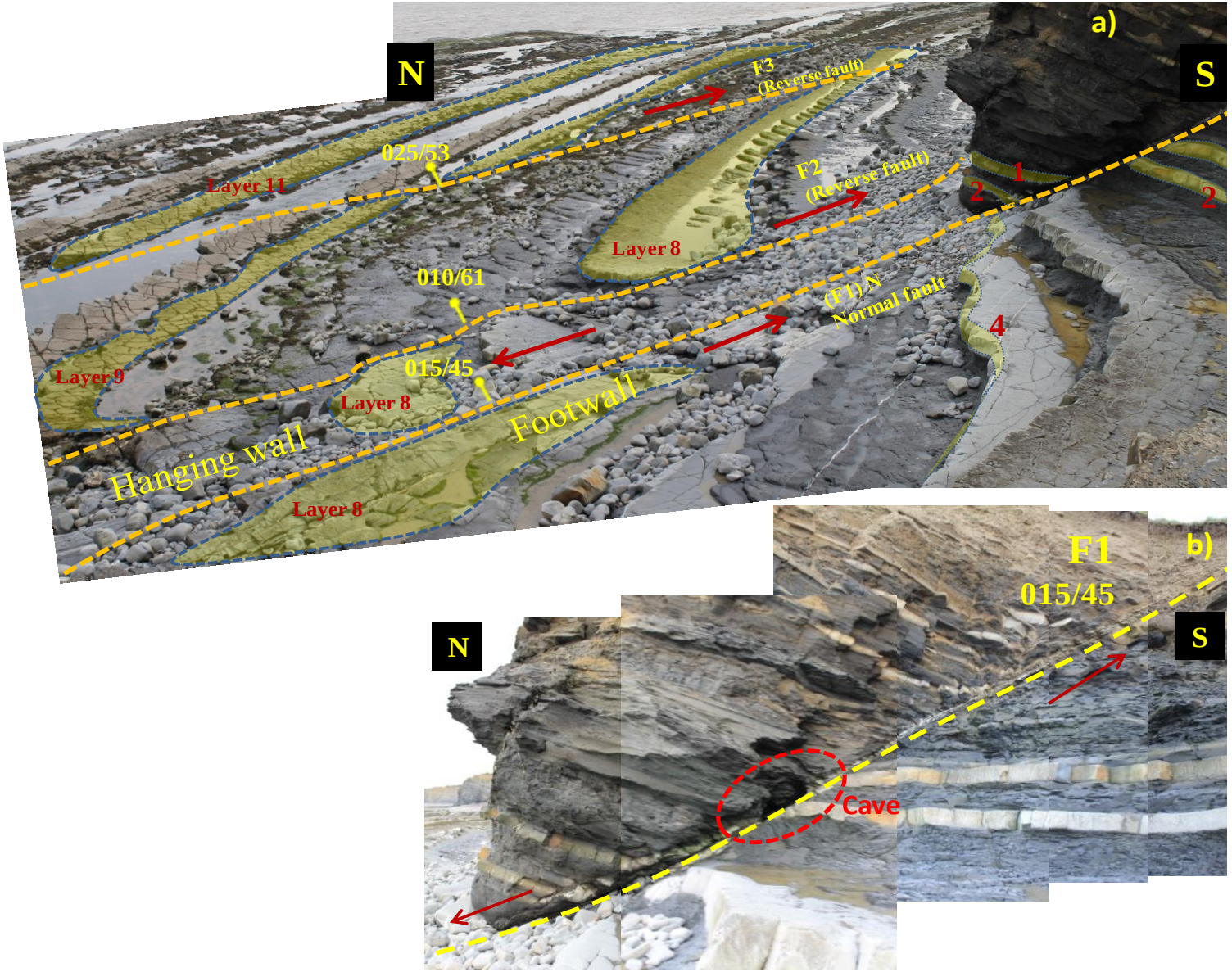

Figure 5.6 a) *Locality 1 Cliff section and beach exposure- F1 &F2and b) Examination in the strike, dip and thickness dimension due to the presence of a cave and in the lower part of the hanging wall good exposure the fault core segmented*

5.1.2 Locality 2 (2 Major Structural Elements –F5-Syncline1 and F12)

This area is about 300 m towards the east (*Figure 5.1*). On the cliff and beach 9 faults have been interpreted, two of them as reverse (F10 and F10 A), Three as minor normal faults (F7, F8 and F11) and two as main normal faults (F5 and F12 respectively- *Figure 5.9*) and near to the one major normal fault (F5) is found a small normal fault (F6) only visible on the beach including that was seen the first Syncline, also, other small normal fault was visualized only on the Beach between 2 minor normal faults (F7 & F8) named F7A . (*Figure 5.8*)

This location was characterized by dominants normal faults E-W striking with an average dip of 65° toward to the north.

5.1.2.1 Locality 2 Layers Description

The rocks hosting the fault exposed on the outcrops consist of organic-rich shale interbedded with limestone, as location 1.

On the cliff, the layers are oriented E-W with a dip average measured between the 12° to 20° towards south in both cases footwall and hanging wall respectively, in addition, some continuity on the bedding was observed related with the fault displacement (*Figure 5.7*).

Multiple Formations of extensional faults, general restricted to 3 steep bedding (dips of 13°-20°, compared with normal dips of less than 10°). The early and listric normal faults are cut by younger steeply dipping normal faults. (*Figure 5.9*)

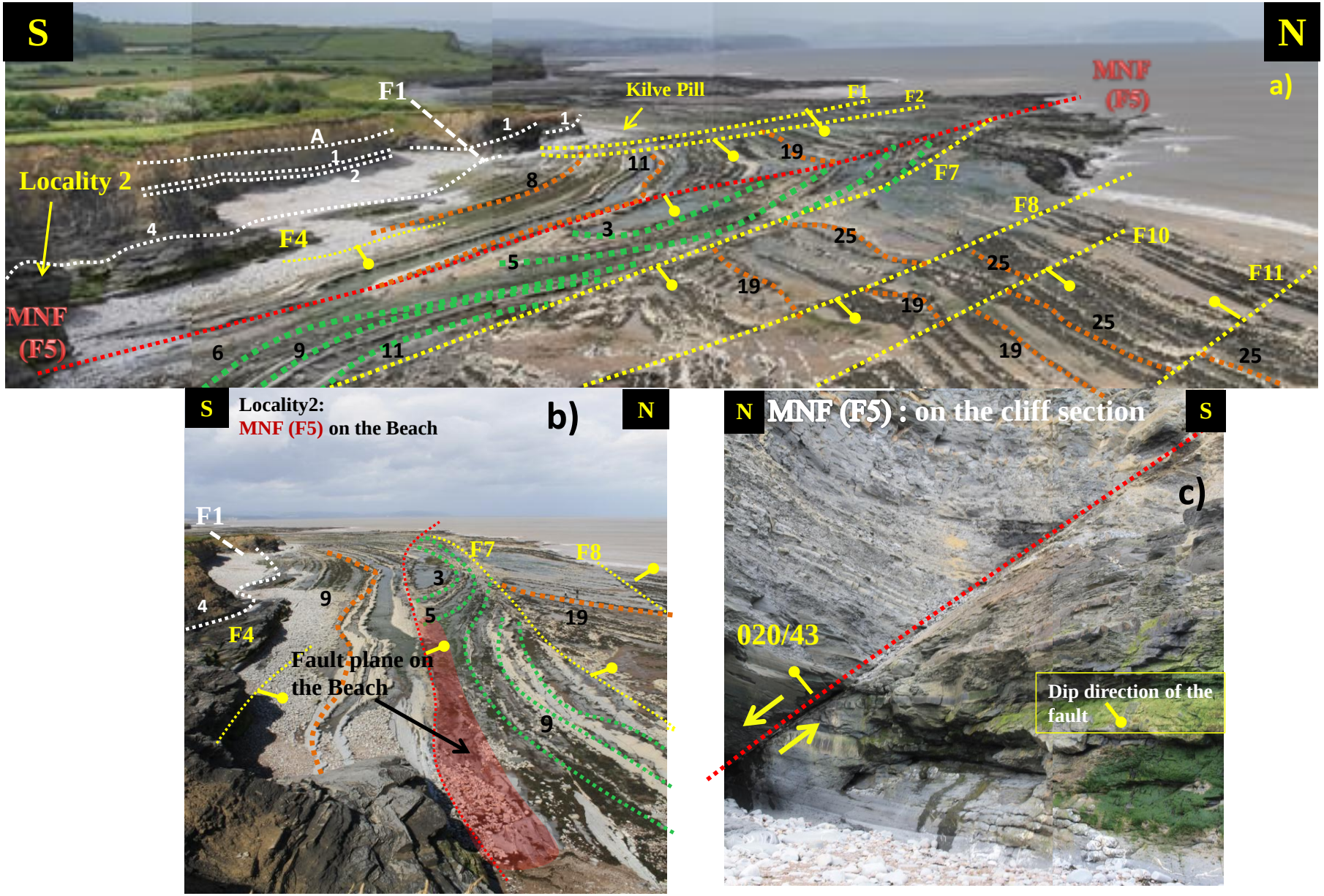

Figure 5.7 *Locality 2-a) Fault interpretations on the beach MNF (F5) and others faults, b) The Syncline 1 seen from the cliff, c) Normal Faults related to the MNF (F5).*

5.1.2.2 Locality 2 Faults Description

Six normal faults were oriented towards the north and two reverse faults with one small normal fault towards the south respectively. *Table 5.1* shows the faults numbers and dip measurements on the location.

Table 5.1 *Comparison of the dips of the south-dipping and north-dipping normal and reverse faults*

Faults	Dip Direction	Fault numbers	Dips (°)		
			Range	Mean	SD
Normal	North	6	43-72	54	12.3
	South	1	-	84	-
Reverse	North	-	-	-	-
	South	2	52-78	63	13

The average dip's faults oriented to the north is between 43° and 73°, and the average dip of the ones oriented to the south is between 52° and 84°. The general striking is NW-SE.

In the fault zone at east of Kilve pill, one of the minor normal fault displacement was measured around 4 m (F7); this was composed of small parallel normal faults (*Figure 5.8*)

In the second major structural element identified as F12 on the East of Kilve pill, the length of the main normal drag was measured using hand tools (i.e. GPS, measuring tape and compass) in the top and base of the cliff section, additionally some the synthetic branches were seen and the measurements were taken from the work done by Kelly, P.G. (1998) (*Figure 5.9*).

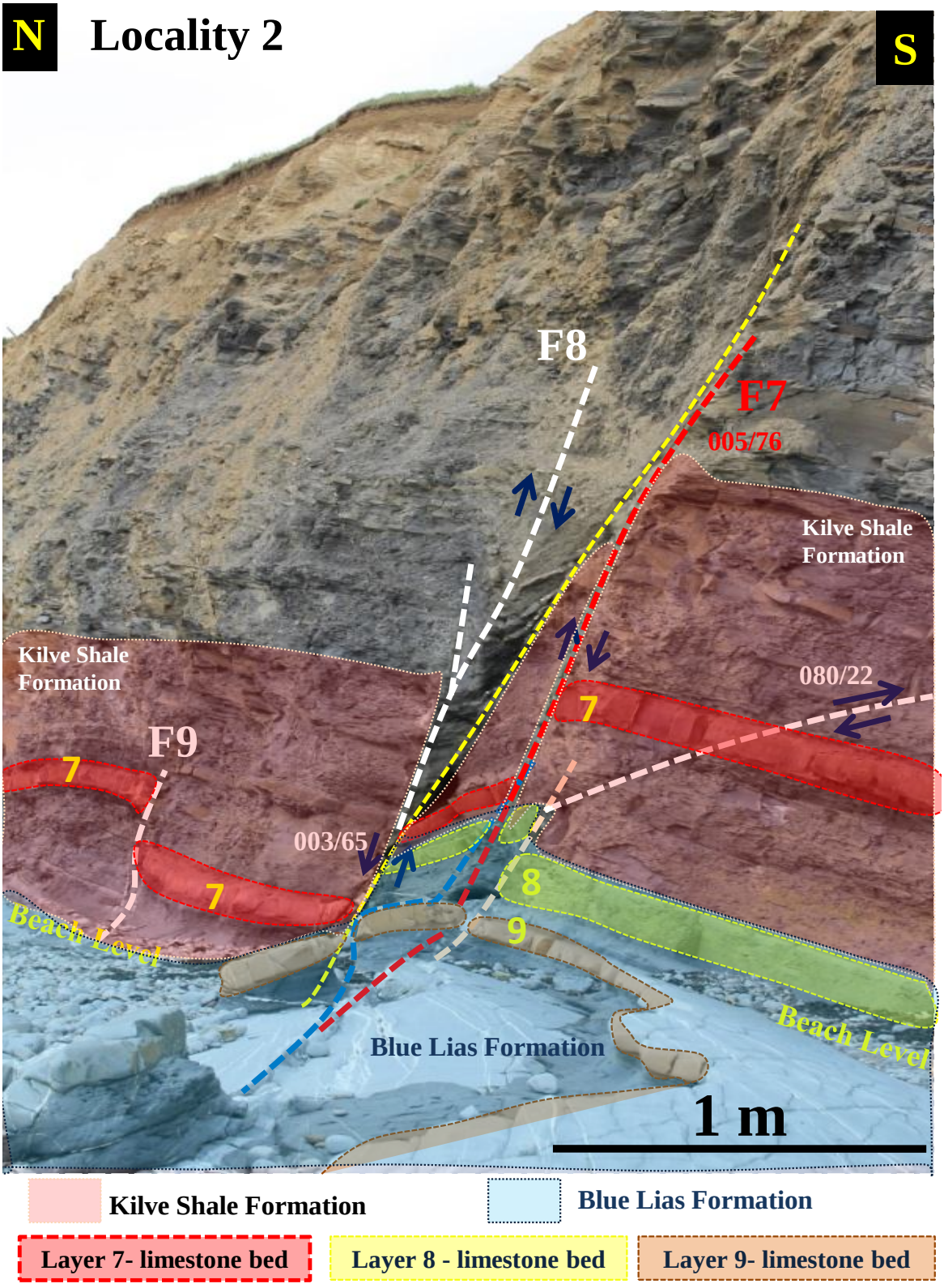

Figure 5.8 *Overview between F7 & F8 interpretation on the cliff*

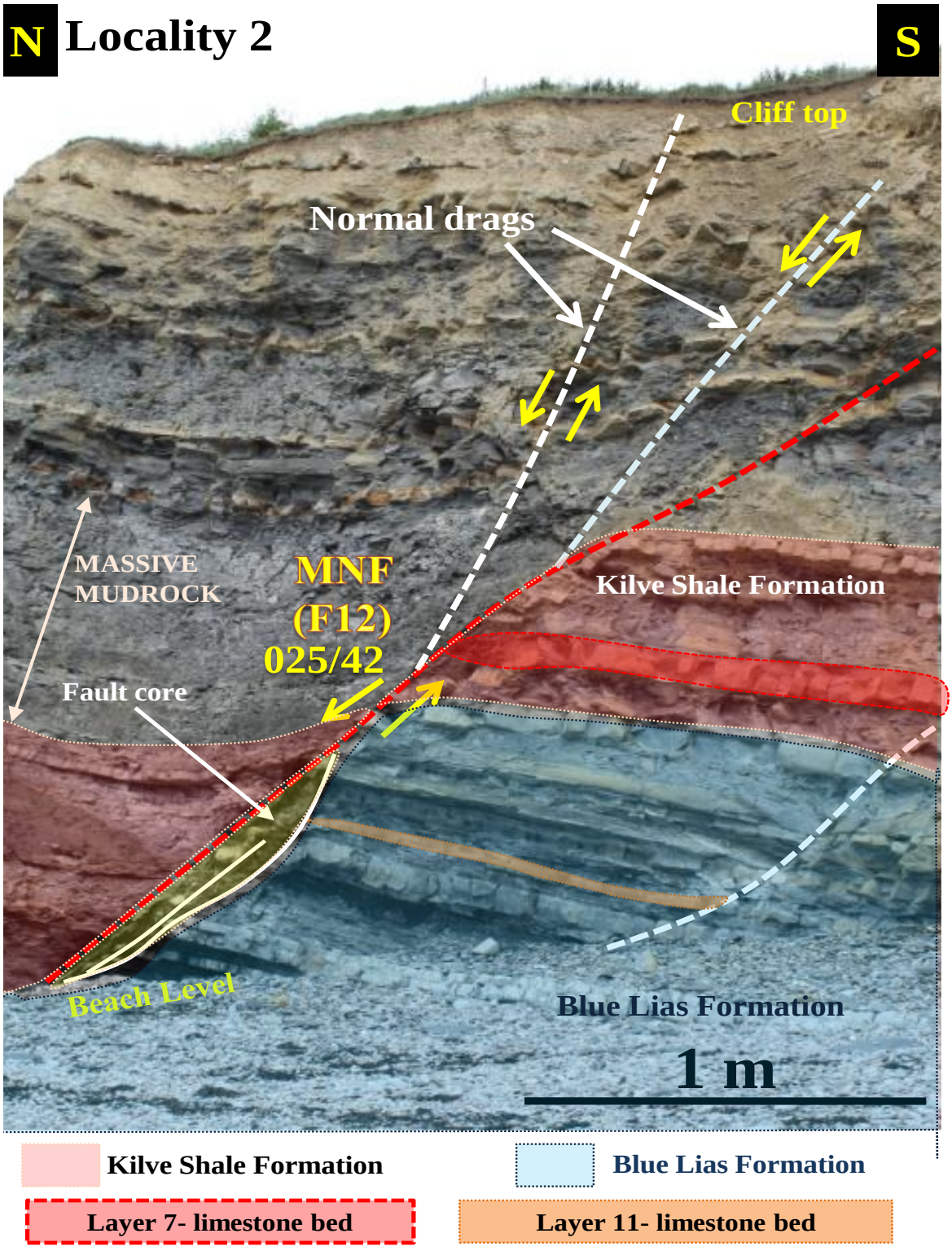

Figure 5.9 *Overview between F12 interpretation on the cliff*

5.1.3 Locality 3 (F15- Syncline 2)

This location is situated about 1.3 Km east of Kilve Pill (locality 1). The location is defined by the main faults F12 (north-dipping) and F15 (south-dipping). The fault and beddings surfaces studied on this locality were well exposed on the outcrops.

In addition, a relay ramp was observed, which was probably broken by normal faults segments (2 faults were interpreted), and previously discussed by Peacock and Sanderson, 1994. They are linked to these symmetric normal fault segments and propagated. The breakage is controlled by bending (curvature), torsion (twisting) and effective tension studied before by Bartley and Glazner (1991) (*Figure 5.8).* From previous works discussed by Peacock and Sanderson, 1994, this relay ramp in the east of Kilve Pill is characterized as stage 3, it involves geometries characterized by fractures (faults and /or veins) cutting across the relay ramp to connect the two overstepping fault segments (*Figure 5.10*).

The bed on the relay ramp observed on the east of Kilve was rotated toward the hanging wall, causing torsion of the ramp, and the displacement seen could cause stresses and in the ramp represented by fold and small fractures. The faults development represents "bookshelf" faulting, accommodating rotation of the axis toward the hanging wall and allowing the extension bedding, also discussed in the literature by Mandl, (1988)

In the location, domes structures were uplifted and according to Conford (2003) these dome in the carbonate pavement were prominent as a result of erosion overlying mudstones unit, but no cross-sections have been found in the current cliff line.

The visible domes structures run towards the north-northeast. These were within the hanging wall of the relative major fault (interpreted as F13) and close to the relay ramp studied by Peacock and Sanderson, (1999) and Bowyer and Kelly, (1995*)* showing that east-west normal faults cutting the Lias on this coast representing the earliest phase of extension.

According to the observations in/on site of the structures (*Figure 5.9*), Fig. B and C, the dome comprise limestone outer shells covering mudstone cores which shows contorned limestones and

shale features without any calcite veins. No macrofossils were seen in the domes. However, some of them were found around the locality (Figure D).

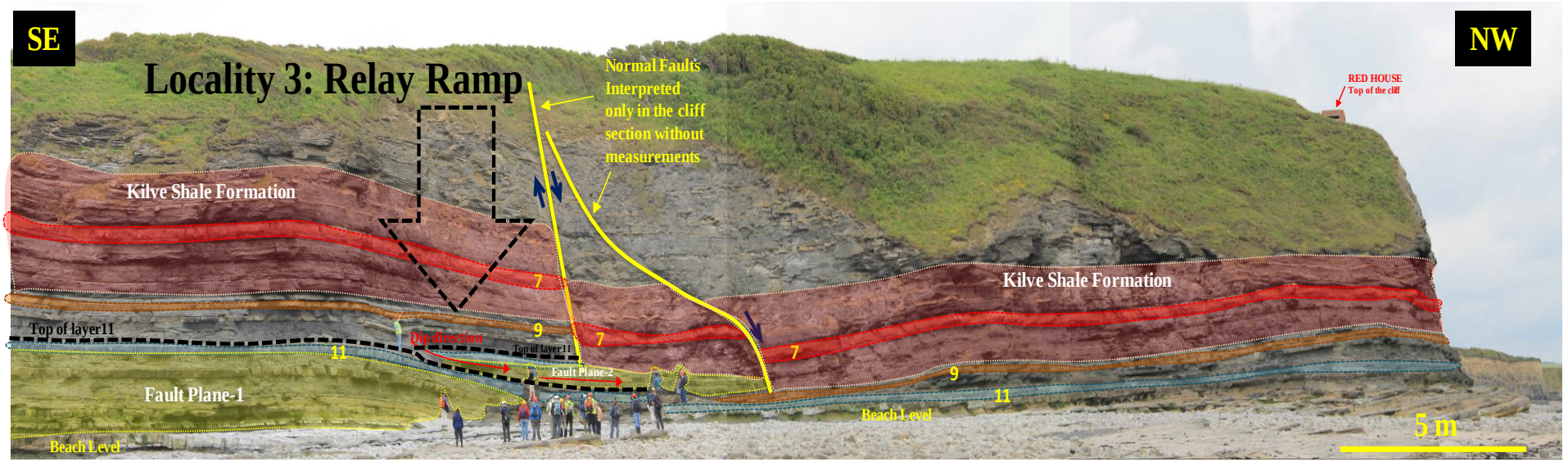

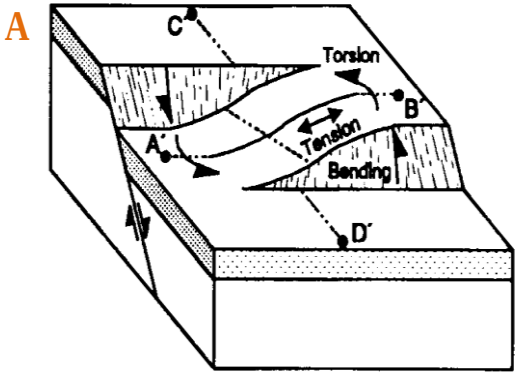

A. Block diagram of two overstepping fault segments after displacement has occurred Both lines have been extended, so effective tension has occurred in the ramp. The rotation of the relay (anticlockwise in this case) about a subvertical axis involves torsion (Bartley and Glazner, 1991)

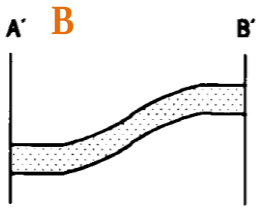

B. Cross section of line A'B' showing the bending of the line in the vertical plane.

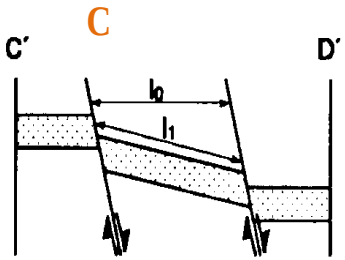

C. Crosssection of line C'D' showing that the ramp has been rotated; this deformation involves torsion about an approximately horizontal axis. The original length of the portion of CD within the ramp (l0) is less than the new length (l1), so bed length tends to increase perpendicular to the strike of the faults, which can be accommodated by veining and/or minor faulting.

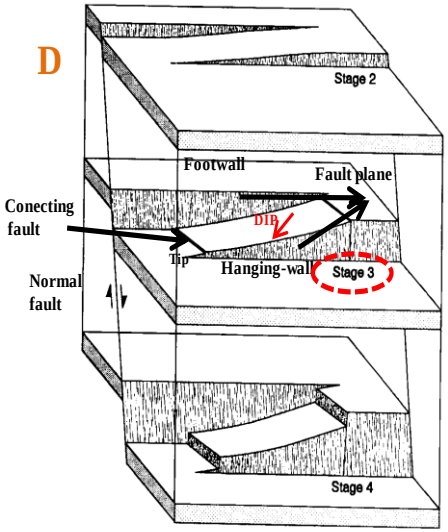

D. Block diagram of the possible spatial distribution of relay ramps (Peacock and Sanderson, 1994)

Figure 5.10 *Relay ramp seen in the locality 3 and diagram taken in account in the interpretation.*

Locality 3: Dome structures and Ammonites

Figure 5.11 *To 1.3 km east to Kilve Pill, direction Lilstock, domes structures and Ammonites.*

5.1.3.1 Locality 3 Layers description

The rocks consist of limestone and shale, in accordance with the description of the previous localitions. From previous works, this locality is characterised by the youngest layers exposure from the Early Liassic sequences.

In the cliff section, the limestone beds were seen as deformed and the thickness was limited (between 5 cm to 20 cm), with predominant shale content, the displacement and dip was difficult to reach and measure.

5.1.3.2 Locality 3 Faults Description

The architecture of the faults on this locality is less complex compared to locality 1 & 2. They were exposed on the cliff and tidal section. (*Figure 5.11)*

The fault planes and fault tips were typically associated with complex zones of fracturing (i.e. on the Relay ramp seen in the locality). The fracturing plays a crucial role in fault development.

Three faults were identified on the area, which could be described by dominants normal faults, striking E-W, and dipping between 55° to 80°. The faults are mainly toward the north, but the the fault interpreted as F15 is toward the south and was used in the model as boundary margin in order to separate with the locality of Early Lias sequences. In addition, the Fault F15 was linked to the second syncline seen in the area (*Figure 5.1)*

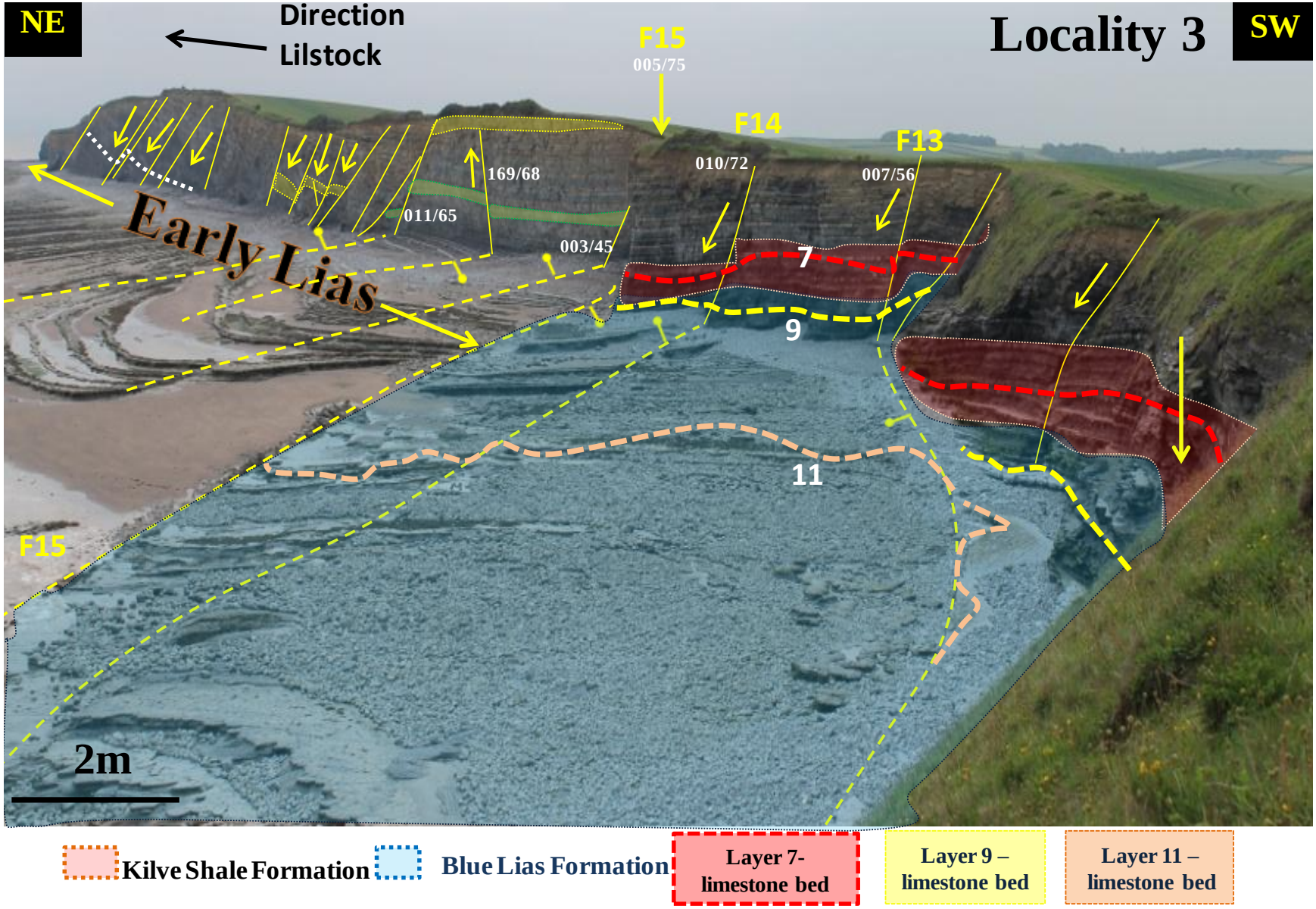

Figure 5.12 *Locality 3: faults interpretation on the beach and cliff section; only 3 faults were integrated in the 3D geological model.(F13, F14 and F15).*

6 Geological Modeling Process

The Petroleum Geologist should organize and interpret the well data, seismic and geological information in order to build a 3D reservoir model. This case study involved data and information taken from outcrops, combined with maps and photographs in order to build a structural and stratigraphy interpretation. In addition, previous works (published and unpublished) realized on the area were taken in account to build a 3D model of the area.

In the structural framework, there are 13 horizons and 12 faults. Information about stratigraphy was included in order to define facies distribution.

6.1 Images Geo-referencing

Fly photographs and satellite images sometimes do not match their location data and information, the same may happen with the maps dataset. For this reason, it is important to match them to real-world coordinates system to be used as base map and visual displays purposes.

The *Figure 6.1* shows the process overview used for geo-referencing. The fly photographs and satellite images were carefully examined and geo-referenced in ARcGIS. The geo-refencing process determined control points that were found in the digital images and helped as guide. The control points were identified on the images and assigned their real-world coordinates (GPS measurements), taking two points in the four corners on the figure as X, Y coordinates, and some more in the middle of the images.

As Resulted, five Images were geo-referenced with appropriate coordinates system for the area in study. (***WGS_1984_Complex_UTM_Zone_30N***- in PETREL)

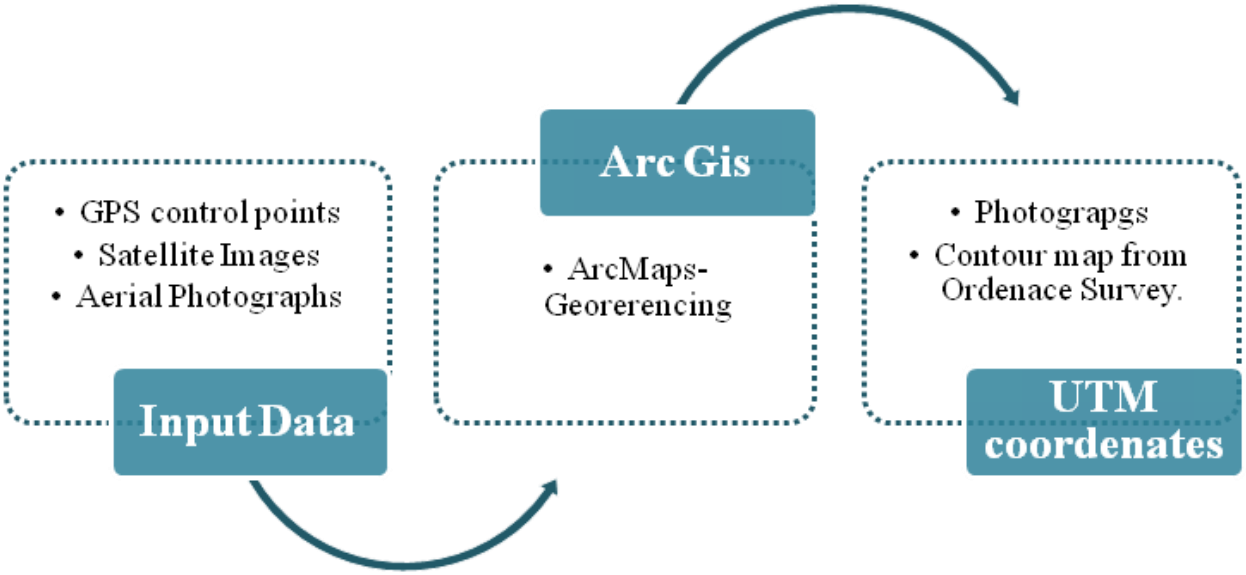

Figure 6.1 *Georefrencing process overview.*

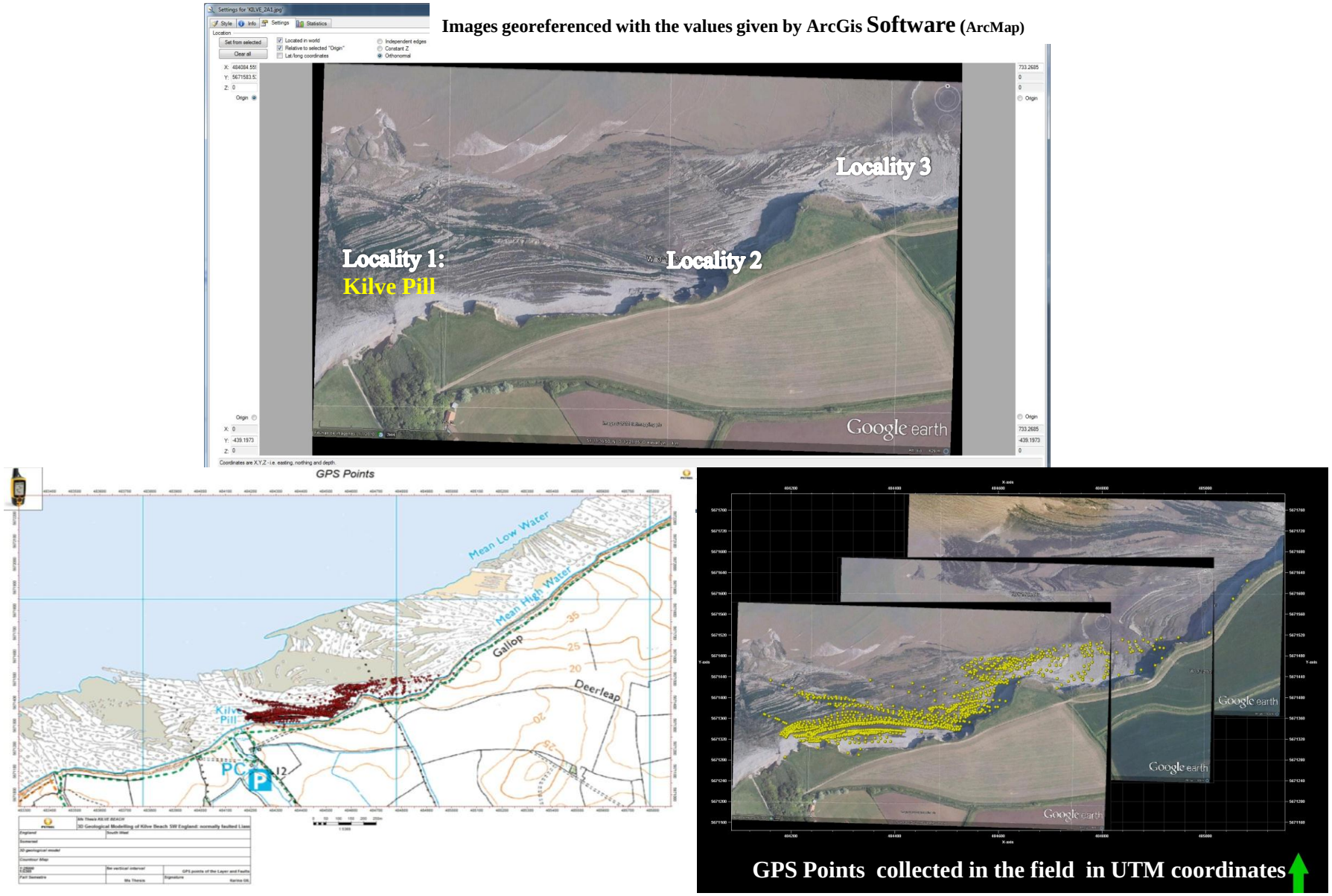

Figure 6.2 *Overview the geo-referencing into Petrel*

6.2 Surface reference data

This section started with the figures geo-referenced which were used as base map. One of them was the contour map which was digitized in Petrel, including its elevation to generate a contour map in 3D and the images to visualize later on, the layers and fault surfaces.

Strike and dip data collected on the field (layer and fault planes) were imported, documented and named according to the fault blocks interpreted on the three locations. The strike and dip data were included in the map. In addition, to build the surface, some dummy points were generated using trigonometry in order to fix the high and orientation of the bedding surface towards to the south, and the fault surface towards to the north. The *Figure 6.2* shows the general schematic of the process followed, while *Figure 6.3* shows the detailed workflow used.

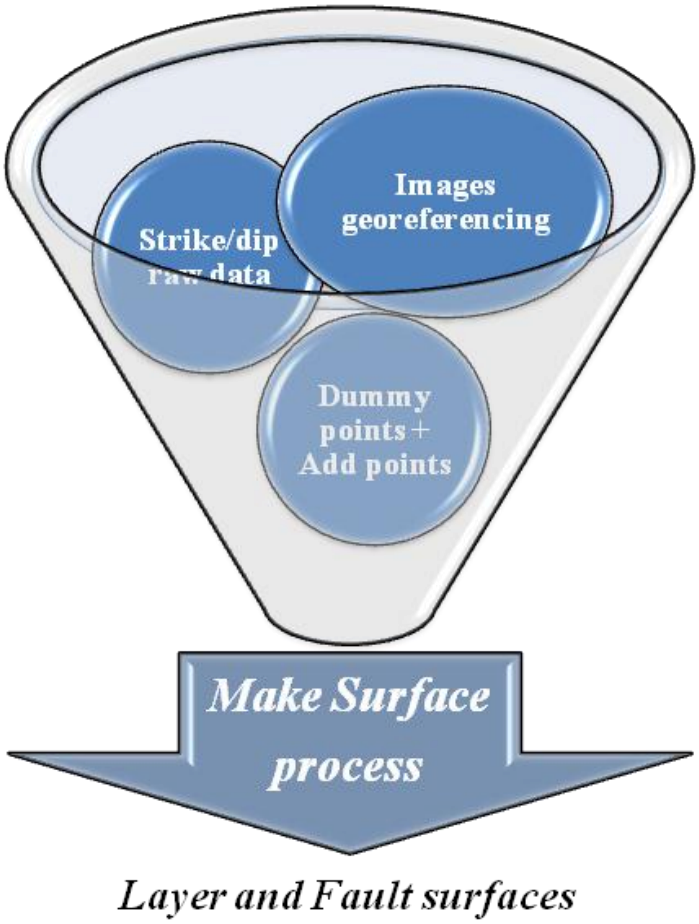

Figure 6.3 *scheme showing the input data filtered in order to generated the horizons and fault surface*

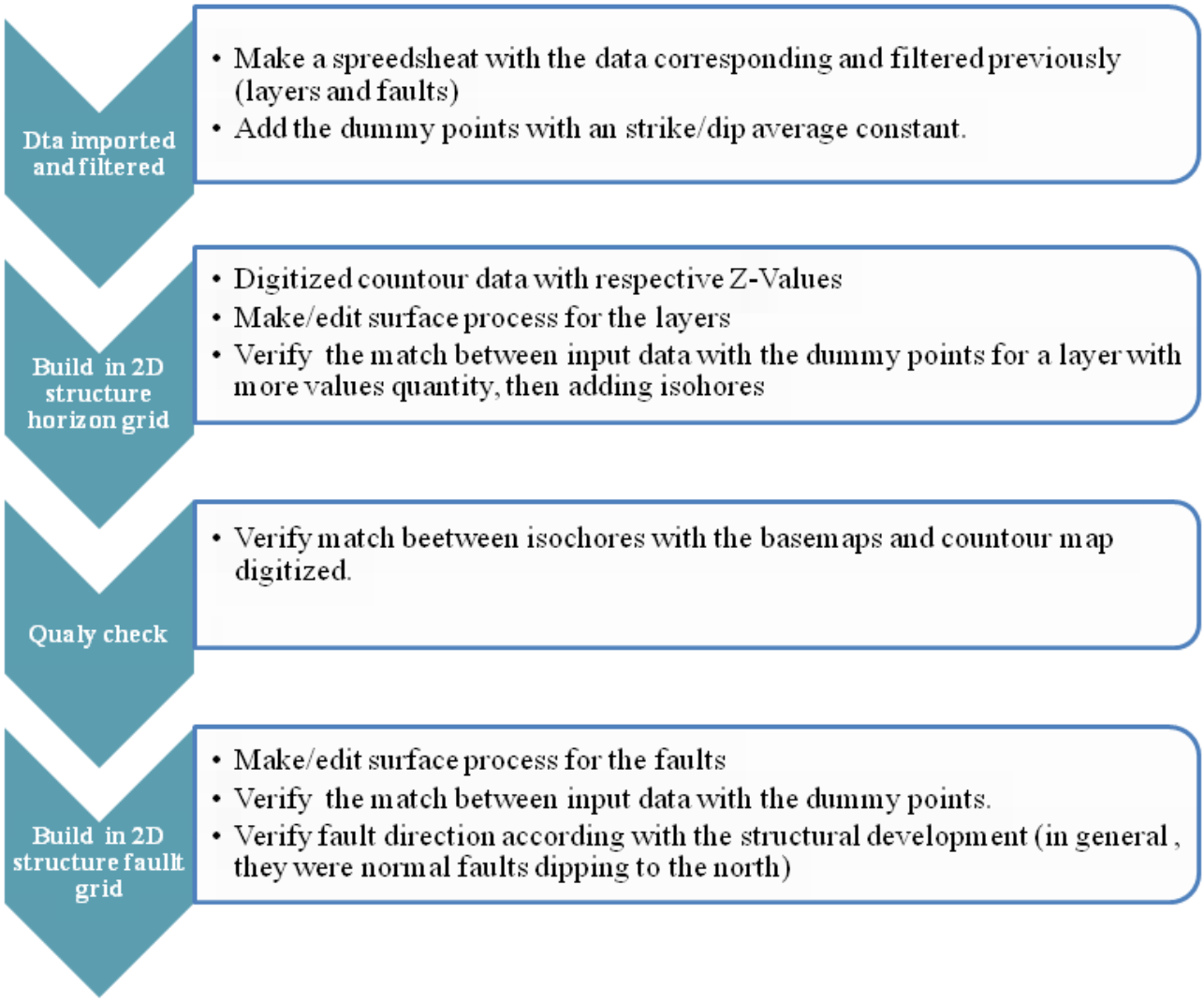

Figure 6.4 *mapping workflow used*

The *Figure 6.6* (taken from Petrel), shows on the top, the fly photo of the locality 1 and 2, the dip of the faults 2 and 5, and the layer 8 dip which goes across both faults. On the bottom left, it is shown the use of the dummy point to generate surfaces, and on the bottom right, the faults 2 and 5 surface, as well as the layer 8 surface.

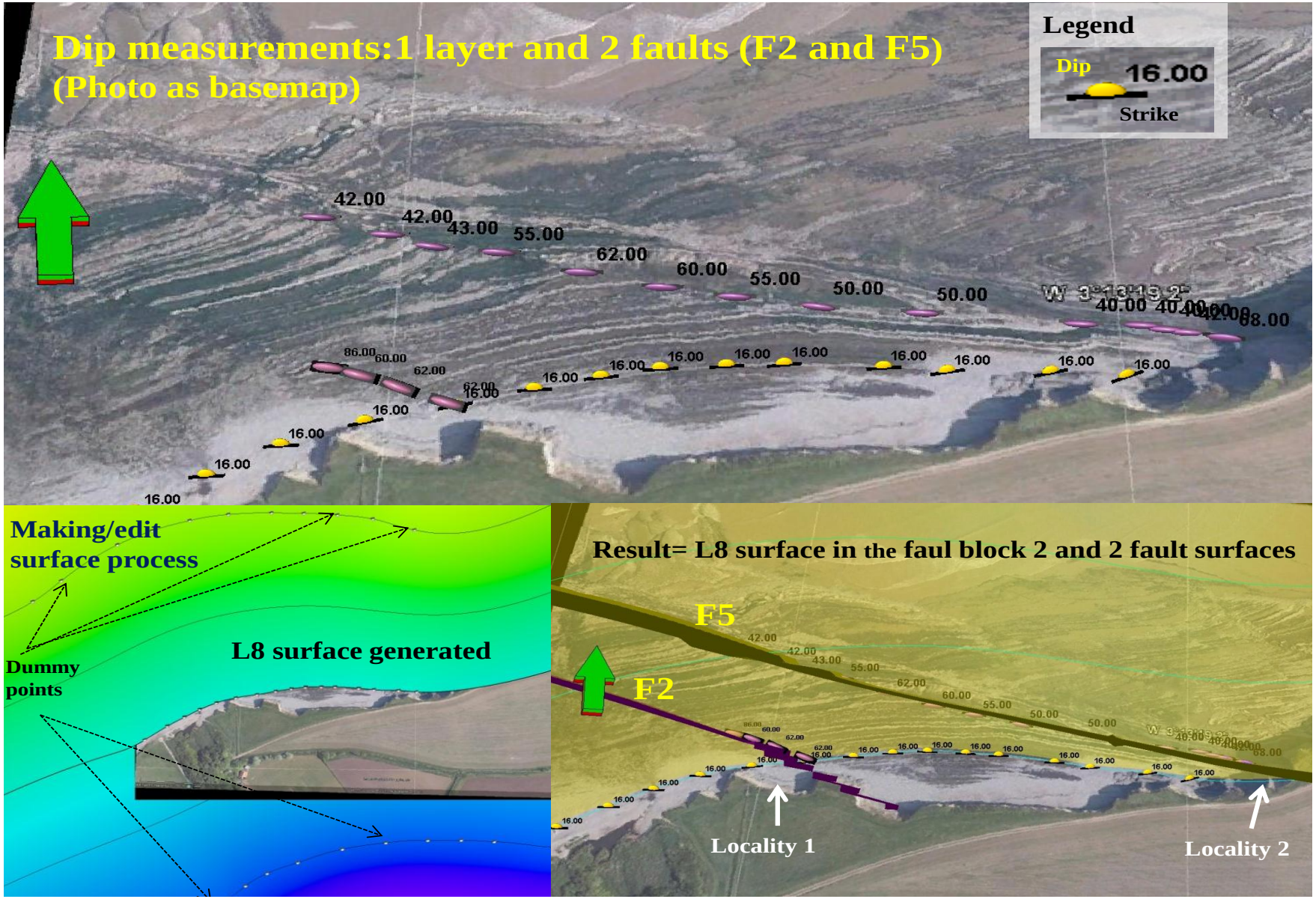

Figure 6.5 *Petrel overview of the layer and fault surface procedure*

The Isochors 3D modeling process was linked together to the layer surfaces previously done. These isochors were checked according to the thickness measured on the field, and their geological relationship following the stratigraphic framework defined above. A dominant horizons and adding isochors with the high respective was done throw all segments in order to visualize the 3D model and the behavior of the correlation between faults and horizons in the Area. The *Figure 6.4* shows the overview of the process used which generate 13 horizons by block.

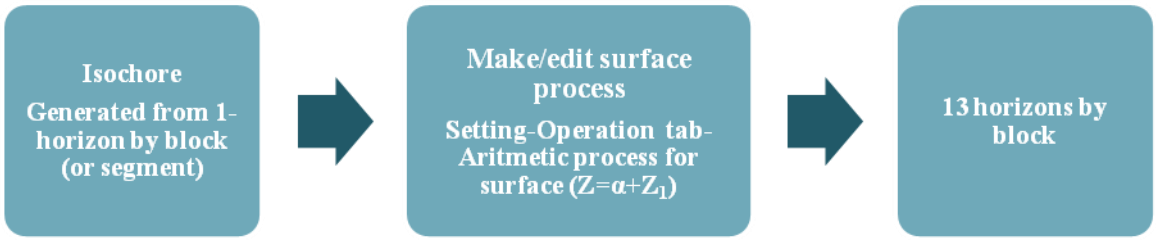

Figure 6.6 *Make surface process*

The *Figure 6.8* shows on the top left the layer 8 surface and the contour map including the fly photograph digitalized, On the top right, the layer 8 surface, the layer 11 isochrones generated the fly photograph digitalized On the bottom left, the layers 8 and 11 surfaces, the fly photograph digitalized and the contour map. And finally at the bottom right, the fly photograph digitalized, indicating the locality 1 and 2, the layer 8 and 11 surface, and the contour map.

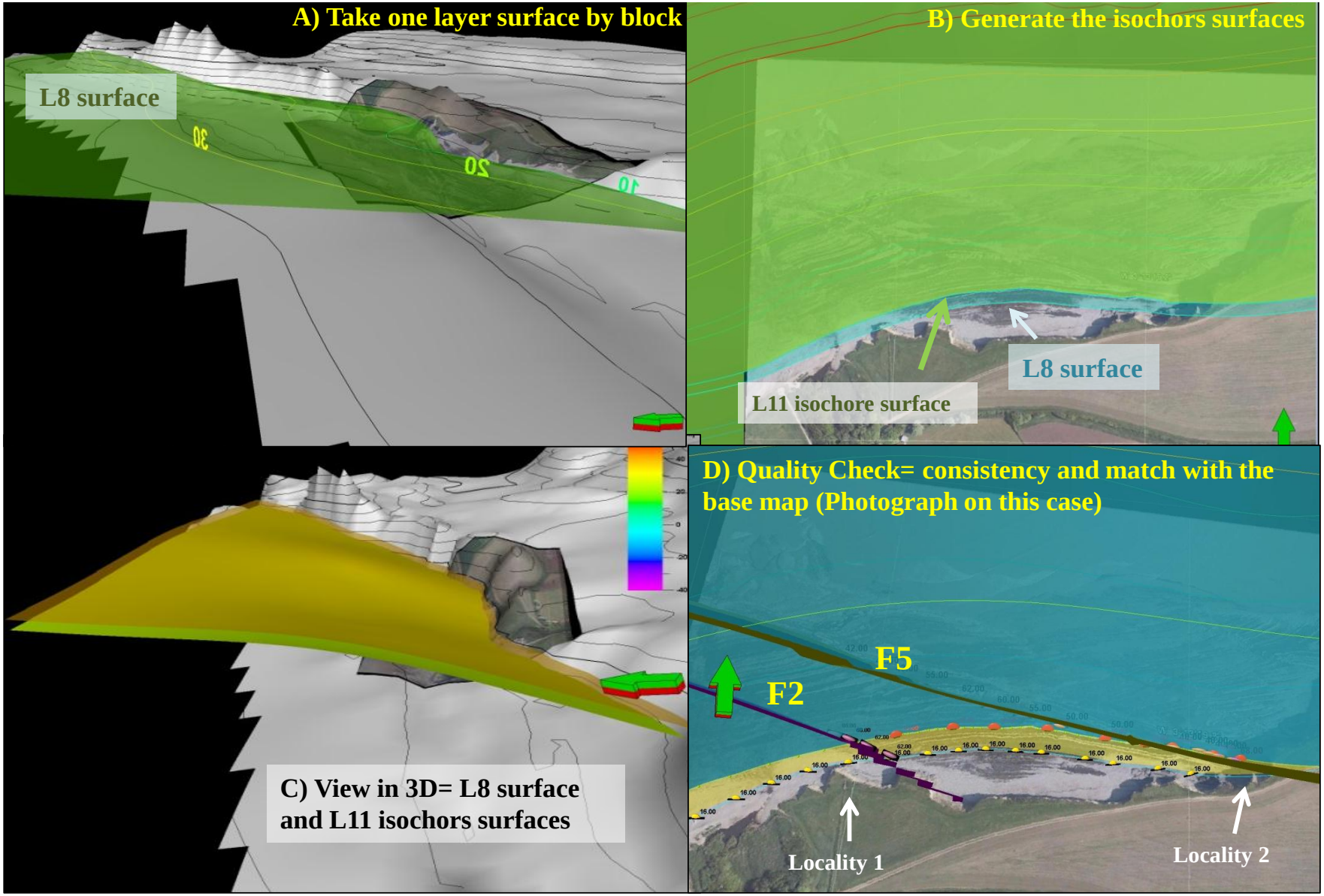

Figure 6.7 *Overview Isochors surfaces process by block*

6.3 Structural Framework

This process enables faults and horizons to be modelled base on the inputs data given. (Petrel Geology-2011). An overview in the volume calculations was included.

The horizon surfaces were chosen from top to down according to the stratigraphic sequences, in addition, strike and dip measured were included. The faults were taken according to the general striking (E-W) and dipping (most of them to the north) and three small reverse faults were integrated to the model.

The fault model was built according to the input data using the grid points imported into *Make surfaces* after these were imported in the "*Fault Modeling*" as straight fault pillars. The overview of the process is shown in the *Figure 6.5.*

The faults surfaces were corrected in terms of faults length, orientation and matching with their respective location into maps and photographs (*Figure 6.6)*

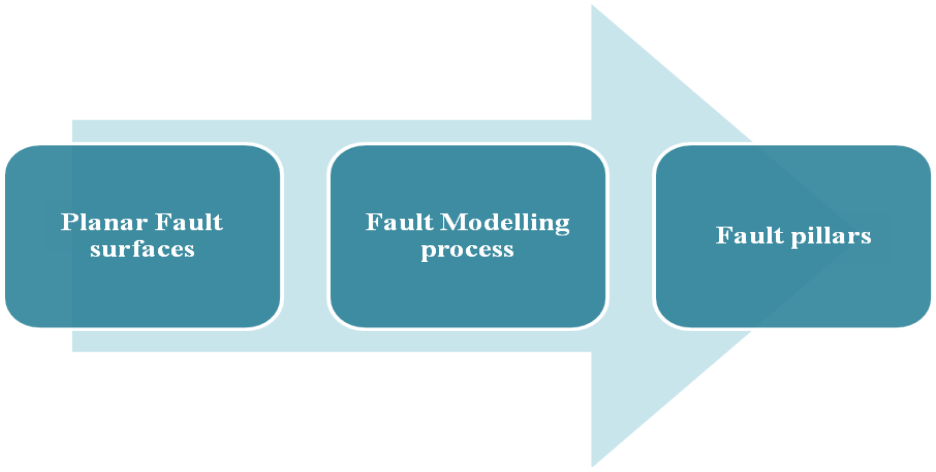

Figure 6.8 Fault Modelling Process

The *Figure 6.10* shows on the top left the F2-F5 and F12 strike/dip measurements digitized on the photographs with their respective surfaces created during the Make surface process, On the top right, The 13 faults pillar generated and merged these with the photographs digitized showing the F3 and F4 connection which was treated as one faults in the structural framework. On the bottom , the two windows' correspond to the quality check on the length and orientation of the fault merged on the photographs digitized.

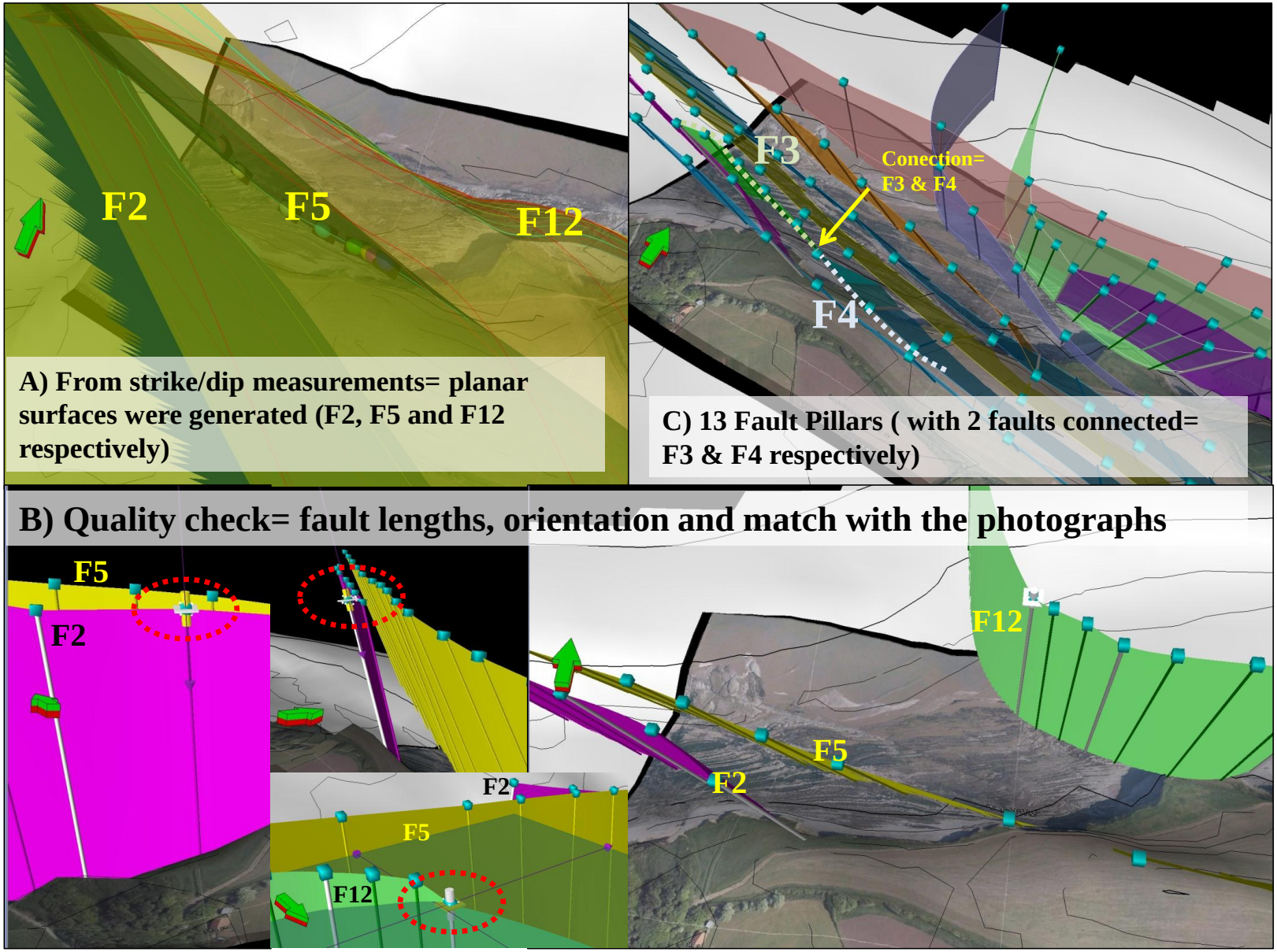

Figure 6.7 *Fault modelling process: Faults (surfaces and pillars), connection and consistency between them*

6.4 Fault diagnosis

In this study the fault diagnosis means to build and checked the quality of the faults as soon as possible in order to speed the QC process. This process involved the fault data as input and its modeling. The fault data point is converted in fault surface and then converted as fault stick or fault polygon.

Into the pillar construction, the fault stick previously generated is the primary input doing a conversion to key pillars that were displayed as X, Y and Z values (point location), it was checked the faults individually passing for the fault block behavior and then verifying the consistency on the all fault modeled in order to gridding these. In the group of fault models, it was checked possible connection between them. Once finalized the QC of all faults a Pillar gridding process as described in the *Figure 6.12 was* started resulting a skeleton in 3D with top-mid and base surfaces.

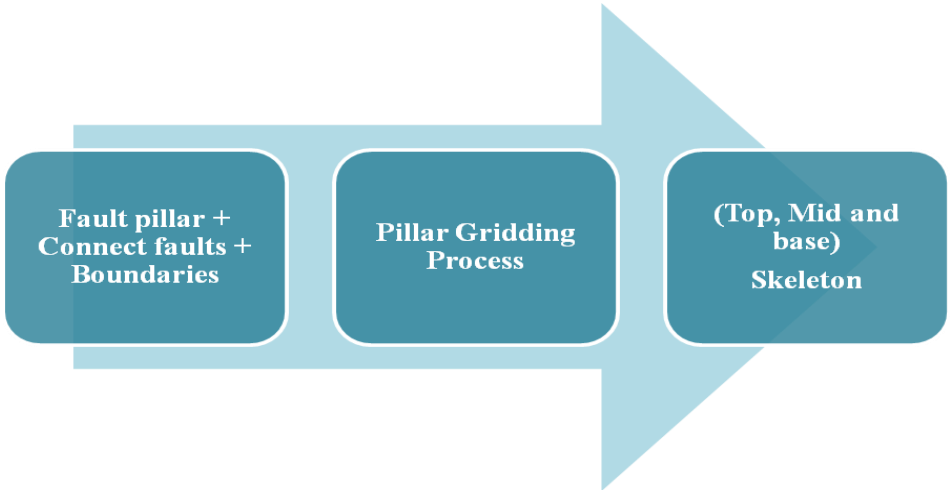

Figure 6.10 *Pillar gridding process*

The *Figure 6.12* shows on the top left the pillar gridding process where the faults interpreted previously were merged in the fly photos checking the trend and connection of the fault on the fly photographs, On the top right, verifying the 13 faults pillar consistency. On the bottom left, the faults saving a good matching with the countour map and photographs digitized. On the bottom right, the model skeleton showing the 3 surfaces that will define the model.

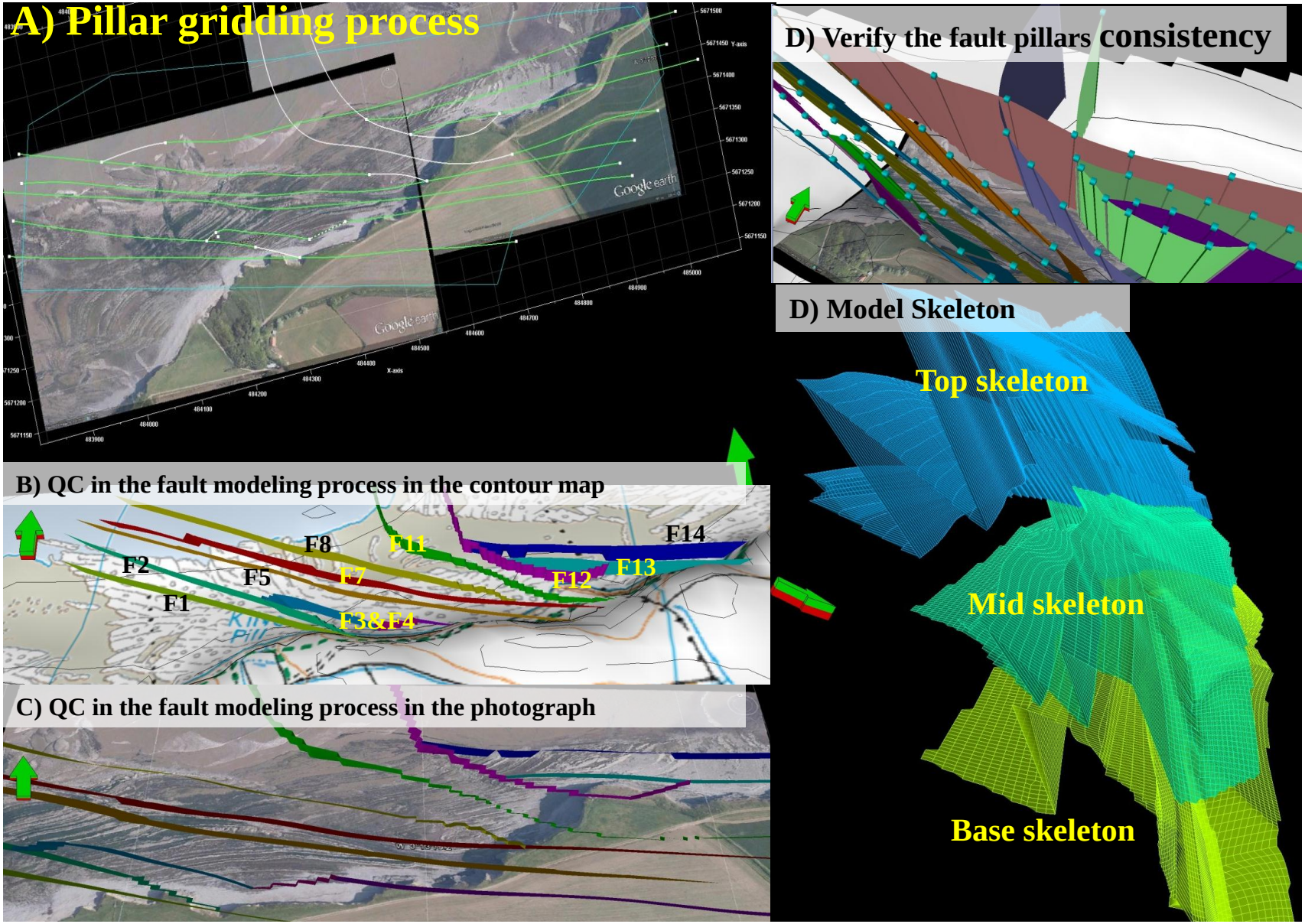

Figure 6.11 *Pillar gridding process: skeleton grid generation base on the key pillar defined in the previous process.*

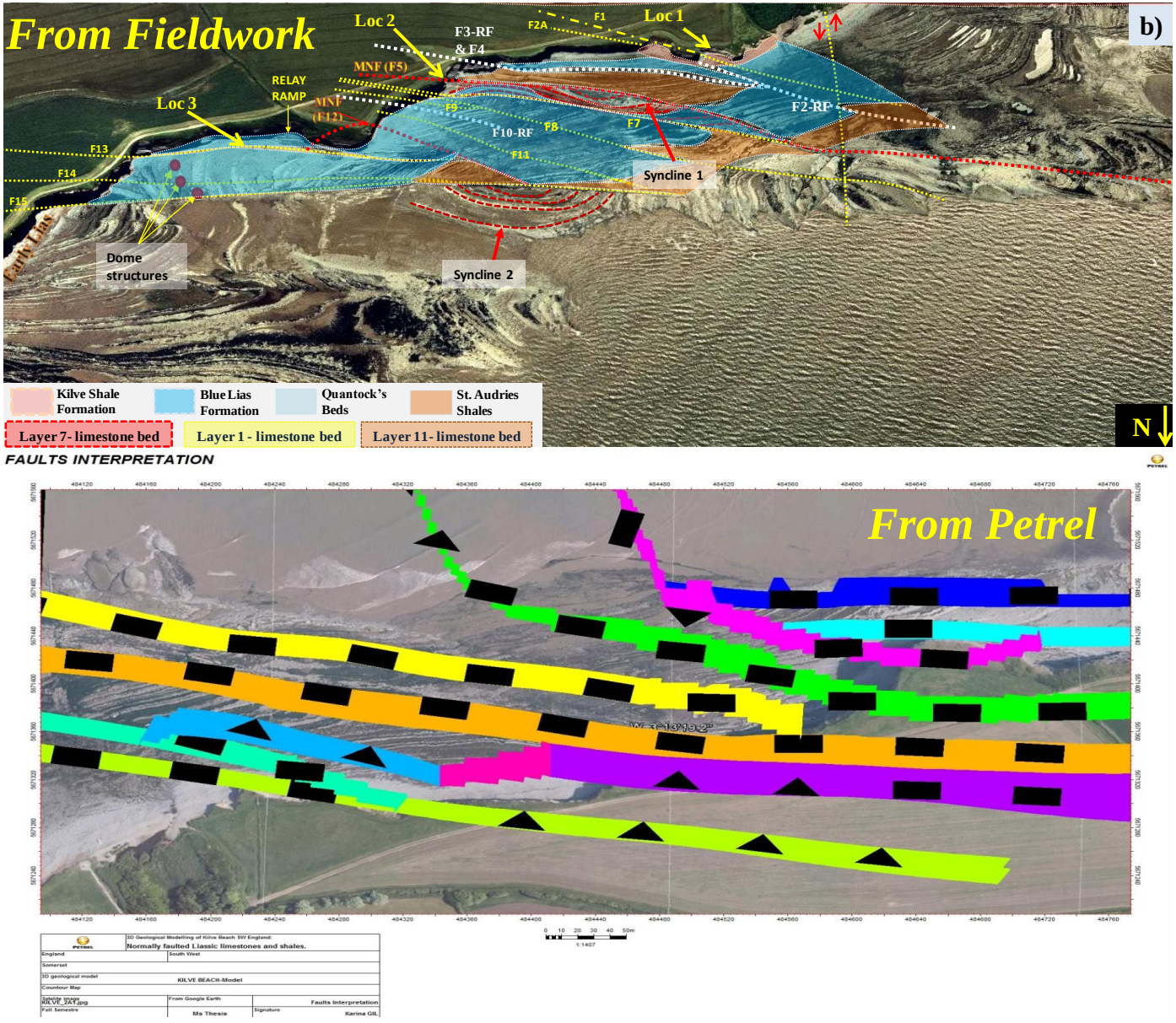

Figure 6.12 *Fault interpretations: good comparison between fieldwork and Petrel. (Checking the god matching)*

6.5 Model Segmentation

The stratigraphic horizons were inserted previously into the 3D model, and the layer surfaces were projected near the faults according to establish in the make horizon process. The layers projections realized by block, was used to show the fault displacement, keeping in mind that the displacements data were not acquired in the fieldwork.

The horizons were selected according to the stratigraphy section (13 horizon surfaces generated by block) and imported into Make horizons process, taking into account the fault modeling and quality check in the input data. The output of the process mentioned above and showed in the *Figure 6.8* were eleven segments

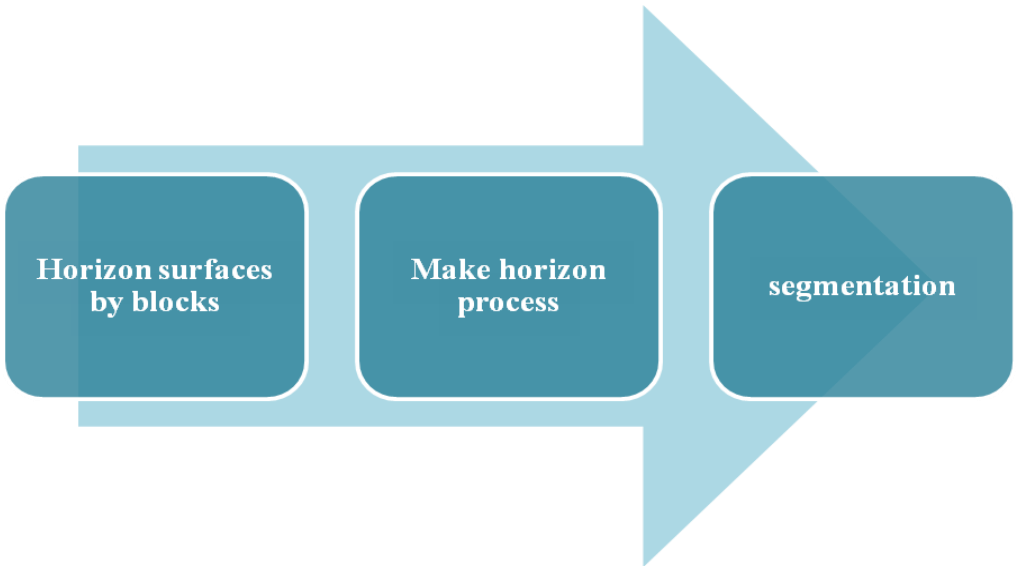

Figure 6.13 *Make horizon process*

The *Figure 6.15* shows on the top, 13 input horizons were identified and located according to their fault block in the input selection. On the bottom, verifying if those input were sorted by the stratigraphy sequences and gave the colour stratigraphy set defined before.

The *Figure 6.16* shows two figures with an overview about the segmentation according to the faults interpreted on the fly photographs digitized.

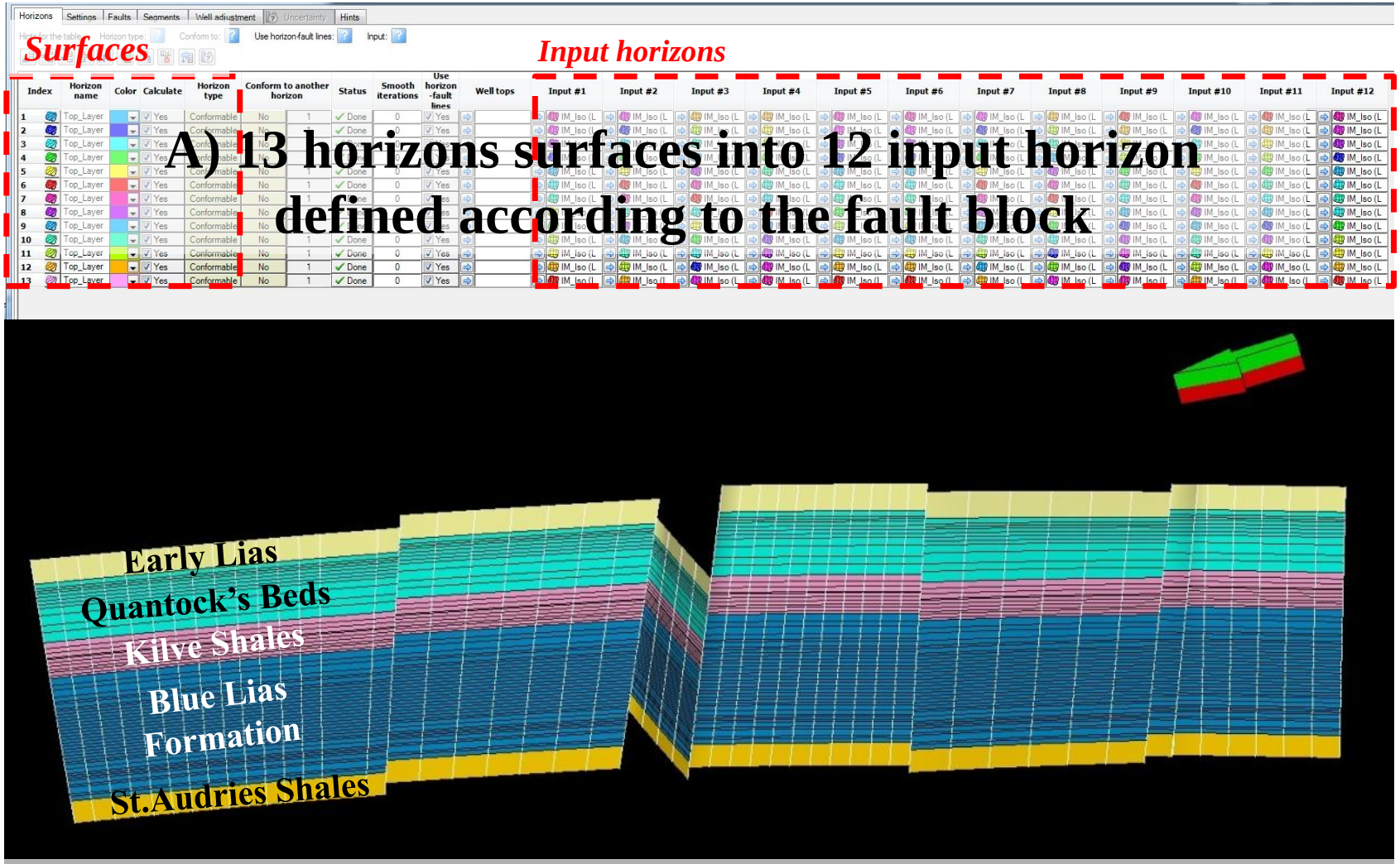

Figure 6.14 *Make horizons process includes interpreted horizons and QC in the stratigraphy show in 3D by intersection (Grid I-direction).*

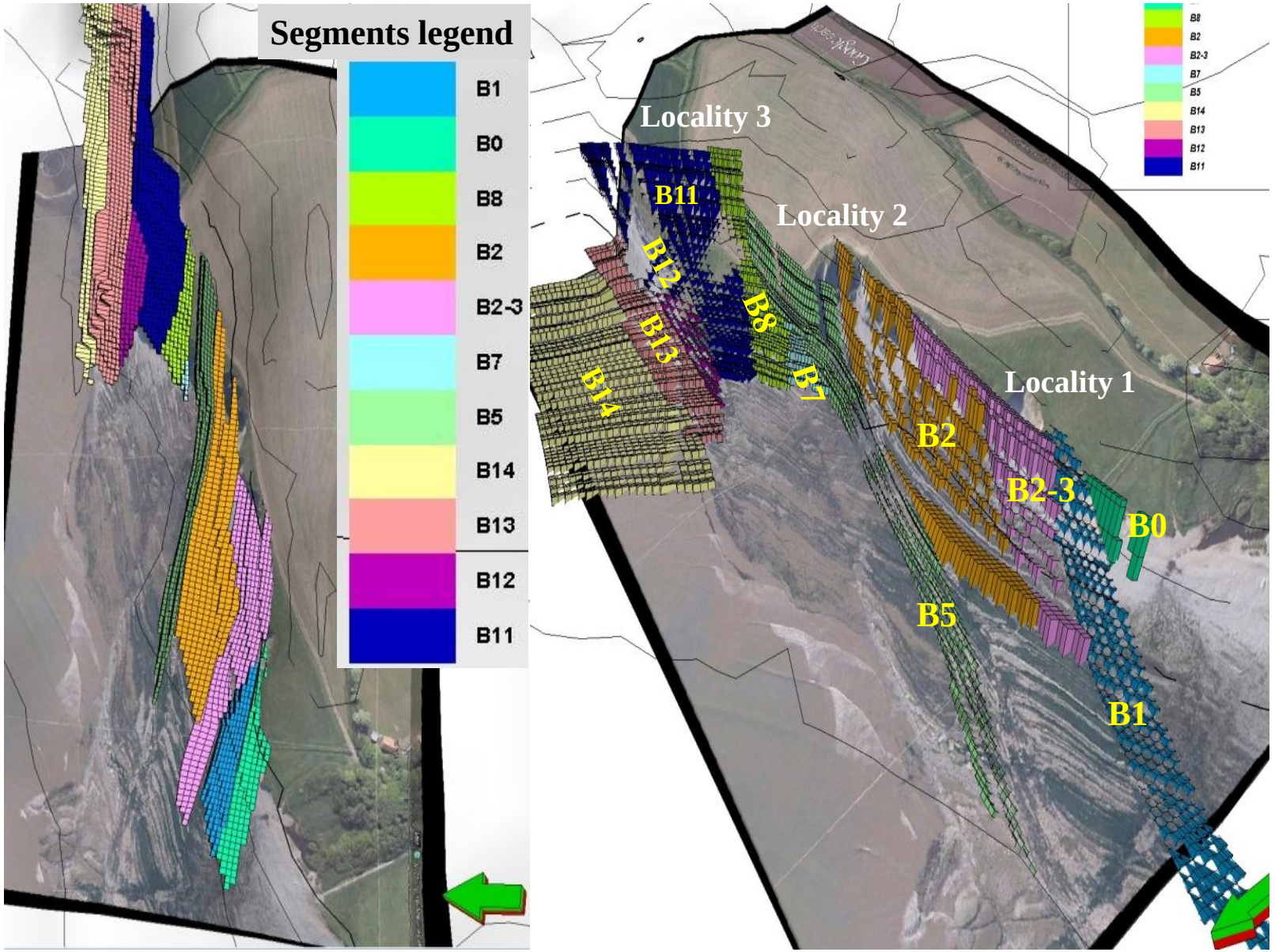

Figure 6.15 *Make horizon process: Overview of Segmentation (done by blocks).*

6.6 Zone Properties and Layering Process

This process was realized in order to create the zones between the horizons and define the vertical resolution in the model. The zones were added according to the thickness of the layer collected on the field (*Figure 6.3 and Figure 6.9)*

It was observed that the thickness of the beds increase towards to eastern (Early Lias formations)

*Figure 6.17*show in detail the Zones and layer distribution. The author made a review in the fault modeling process to visualize the behavior of the layers. In addition, it was checked the pillar gridding process to improve the model.

The quality check of the final 3D model was made by comparing the horizons the ones simulated and the input data.

The final step of the structural framework was the layering process. It was implemented in order to refine the grid by specifying the number of layers by zone division, following the top of the zone (not included input data). The table 6.*1 show* a statistic for Kilve Beach 3D model.

The *Figure 6.17*shows on the left, an example the layer list to make zones with their respective thickness value. On the right, verifying if those zone input was divided according to the stratigraphy.

Table 6.2 *Kilve grid Statistics*

Axis	Min	Max	Delta
X	483759.21	485024.96	1265.75
Y	5671179.64	5671645.38	465.74
Elevation depth [m]	-59.43	121.58	181.00
Lat	~51°11'N	~51°11'N	~0°00'
Long	~3°13'W	~3°12'W	~0°01'

Description	Value
Number of iconized horizons:	60
Number of iconized zones:	14
Number of faults:	12
Number of segments:	11
Number of properties:	13
Grid cells (nI x nJ x nGridLayers)	235 x 79 x 59
Grid nodes (nI x nJ x nGridLayers)	236 x 80 x 60
Total number of 3D grid cells:	1095335
Total number of 3D grid nodes:	1132800
Number of geological horizons:	60
Number of geological layers:	59
Geometry overview:	
Vertical pillars:	0.00%
Linear pillars:	56.55%
Listric pillars:	43.45%

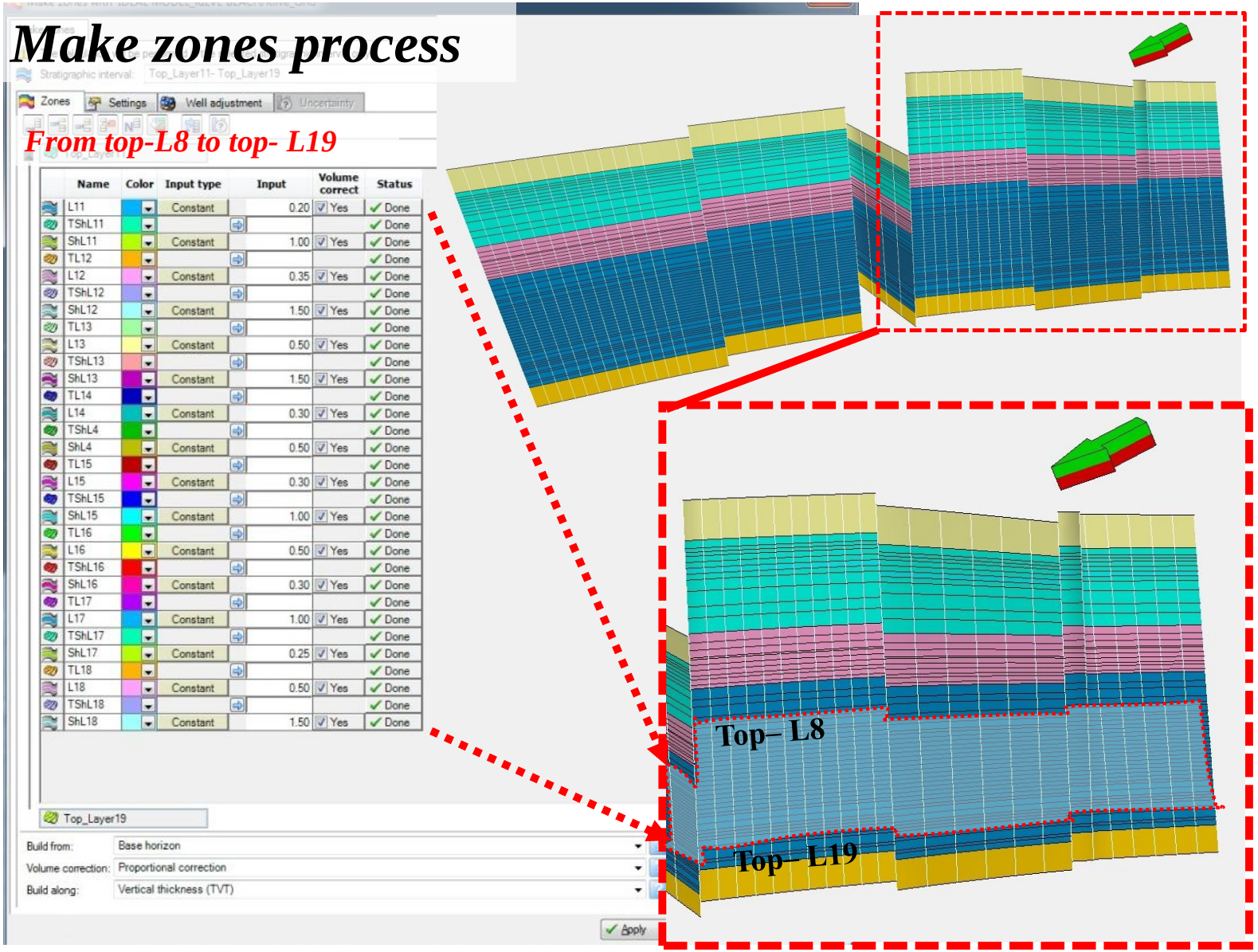

Figure 6.16*Make zones process showing from top-L8 and top-L19 inserted geological zones in the stratigraphic intervals.*

6.7 Property Modeling

This process was the distribution of the continuous (petrophysic) and discrete (facies) properties in the 3D grid. The process was split in three sections

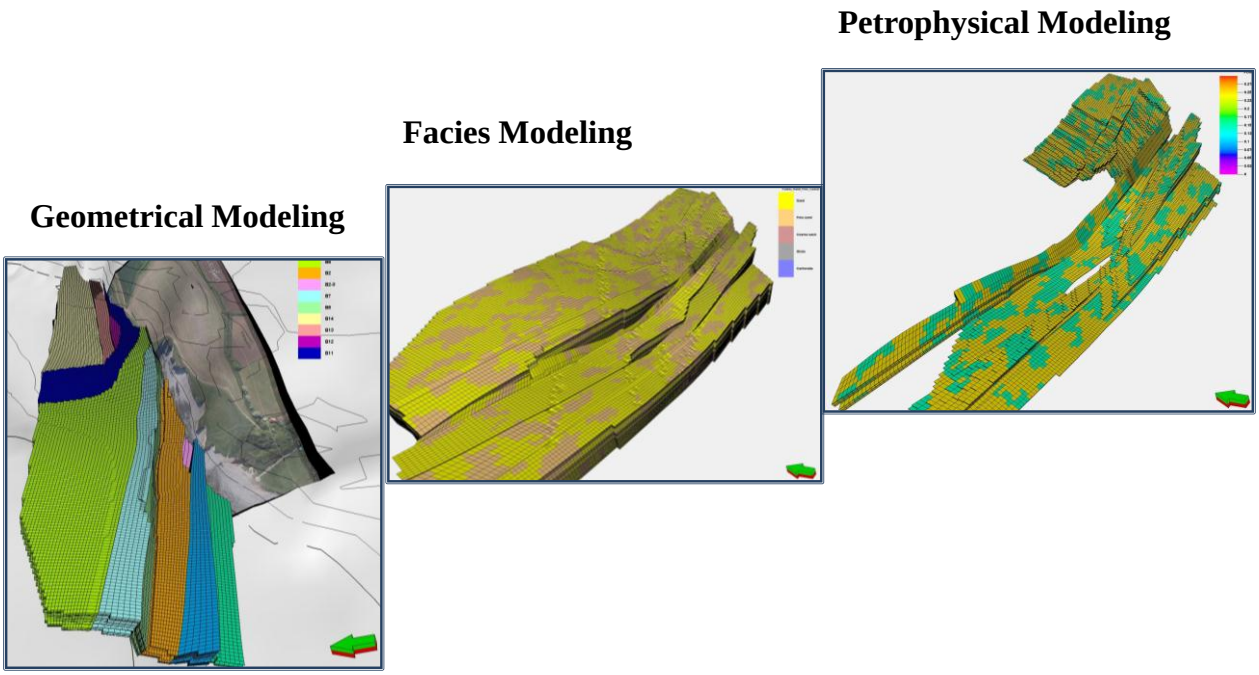

Figure 6.17 *Property Modeling scheme*

6.7.1 Geometrical Modeling

Zones and segmentations were the properties generated on this section. These properties were important for the volume calculation, also, in the facies and petrophysical properties operations.

6.7.2 Facies Modelling

A basic facies model was built conditioned to the outcrops observations (Limestone and shale) represented by two models using the method sequential indicator simulation (SIS) in Petrel.

- Model 1: Sand and shale only
- Model 2: Using fine Sand, Coarse sand and shale facies

The variogram setting for both models was specified with the parameters show in the table below for the sand facies while that for shale was assigned “0” value.

Table 6.1 *Variogram setting for the sand facies.*

	Major dir. Range	Minor Dir. Range	Vertical Range	Azimuth
Sand	**50**	**50**	**10**	**16**

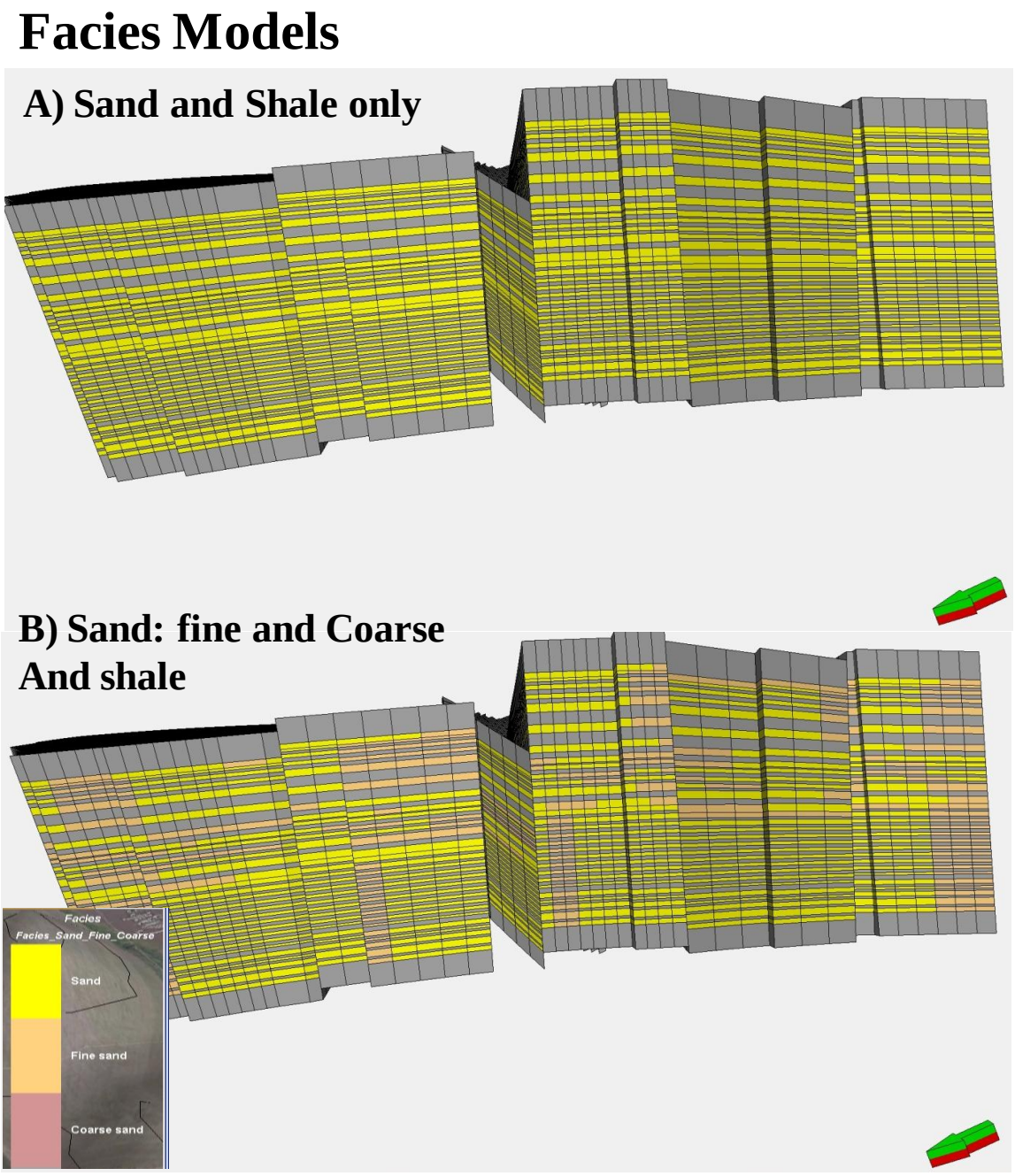

Figure 6.18 *QC the facies models generated*

6.7.3 Petrophysical Modeling

According to the facies properties, porosity, permeability and water saturations were assigned.

6.7.4 Contacts and Volumens

The GOC were defined at -10 m below to the base map surface and the volume in place was calculated.

The *Figure 6.20* shows on the left, the connected volume visualization distributed by colour according to the number of layer assigned in the layering process. On the right, the facie property using the model-2 for the visualization.

The *Figure 6.21* shows the petrophysical and fluid properties generated and merged on the fly photograps.

The *Figure 6.22* shows the volume result spread sheet

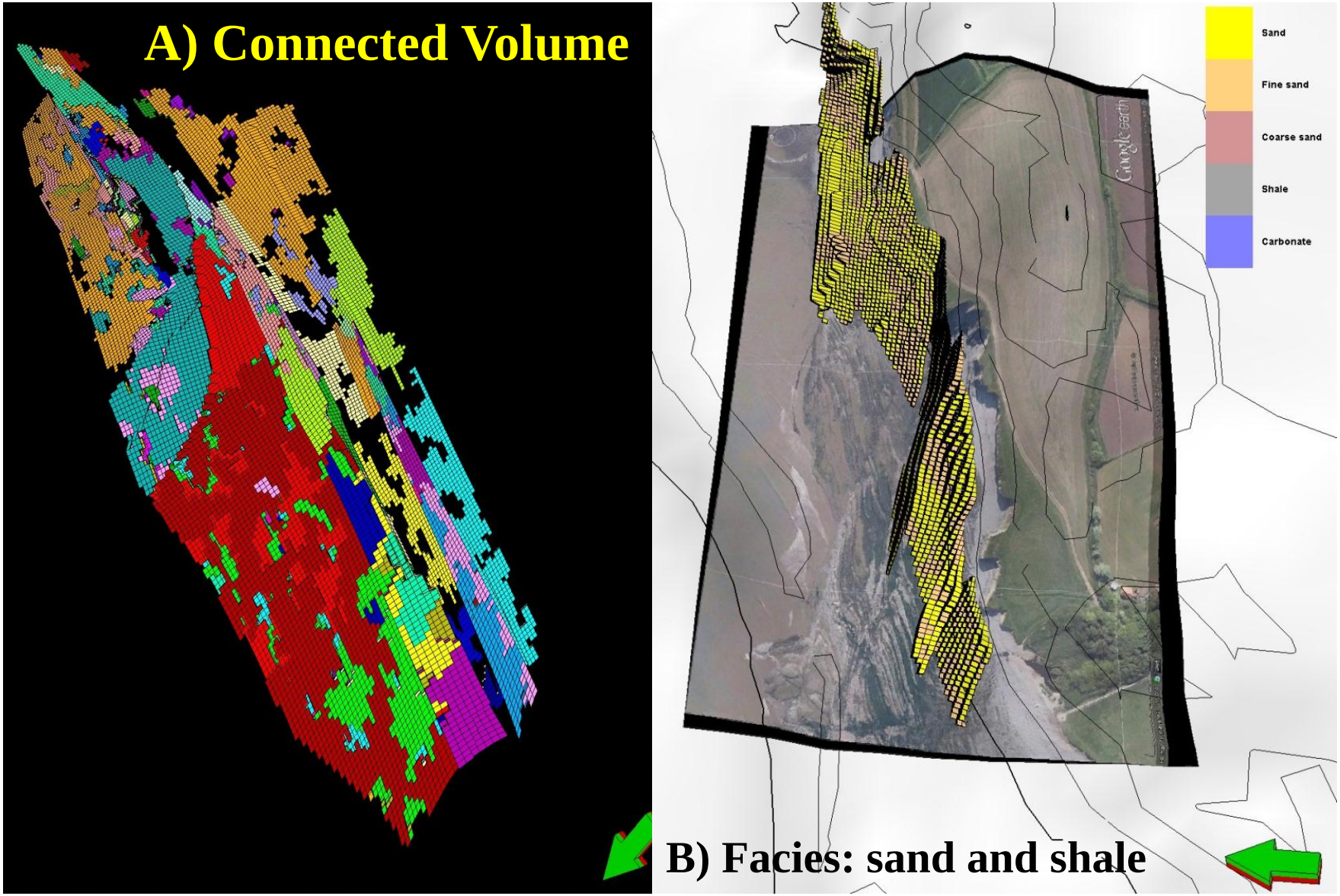

Figure 6.19 *Geometrical modelling showing in 3D view: connected volume and facies property generated*

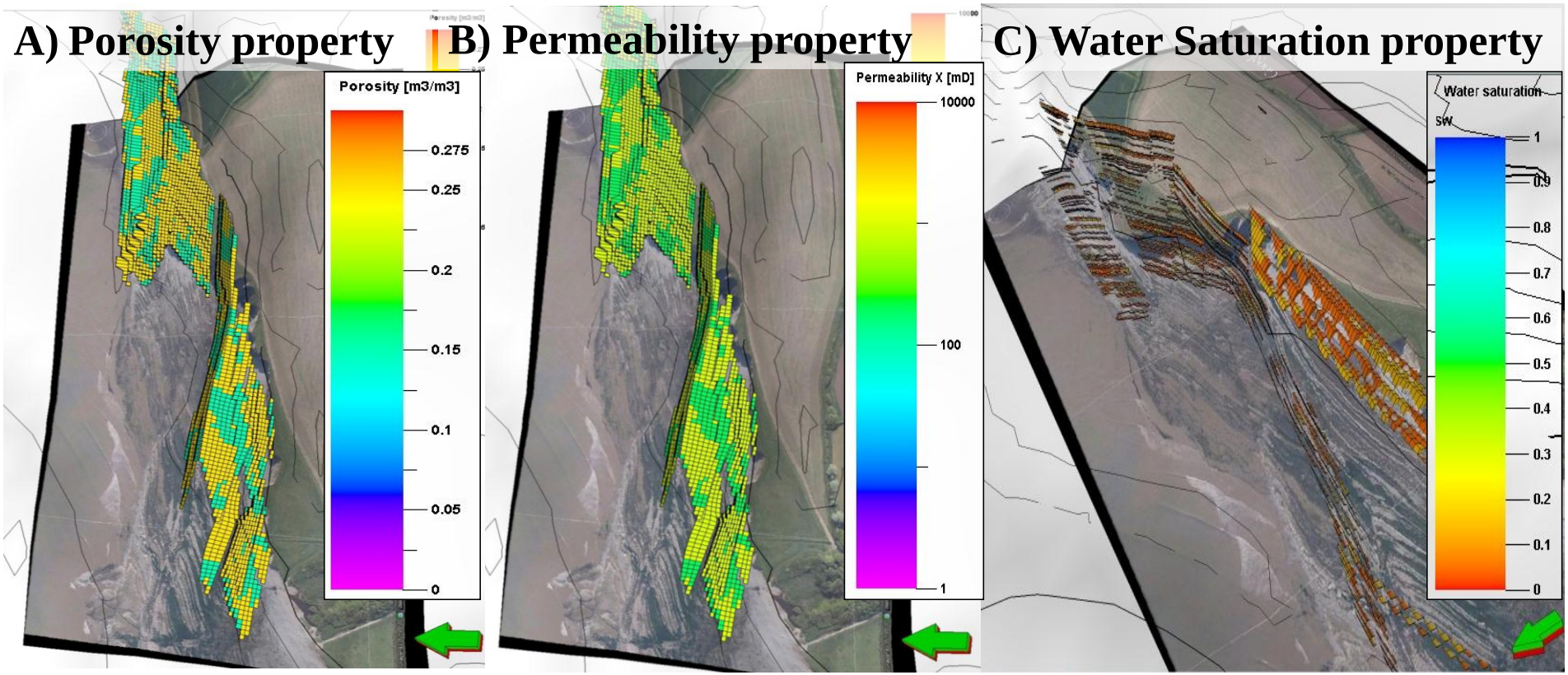

Figure 6.20 *Petrophysical and fluid properties*

Petrel 2011.2 (64-bit)	Schlumberger												
User name	I0281703												
Date	Fall semestre, 2012												
Project	kilve_VOLUMENS.pet												
Model	MODEL_KILVE BEACH												
Grid	Kilve_Grid												
Input XY unit	m												
Input Z unit	m												
HC intervals	Includes gas interval only.												
Upper gas contact:	Contact set\GWC												
General properties													
Porosity:	PORO												
Net gross:	1.00000000												
Properties in gas interval													
Sat. water:	SW												
Sat. gas:	1-Sw-So												
Sat. oil:	0.00000000												
Bg (formation vol. factor):	0.00020000	[rm3/sm3]											
Rv (vaporized oil/gas ratio):	0.00000000	[sm3/sm3]											
Recovery factor gas:	1.00000000												
Properties in oil interval													
Bo (formation vol. factor):	1.00000000	[rm3/sm3]											
Rs (solution gas/oil ratio):	0.00000000	[sm3/sm3]											
Recovery factor oil:	1.00000000												
Case	Bulk volume	Net volume[	Pore volume	HCPV oil[*10	HCPV gas[*1	STOIIP (in oil	STOIIP (in ga	STOIIP[*10^6	GIIP (in gas)[	GIIP (in oil)[	GIIP[*10^6 sr	Recoverable	Recoverable
Case	3	3	0	0	0	0	0	0	668	0	668	0	668
Segments													
B1	0	0	0	0	0	0	0	0	9	0	9	0	9
B0	1	1	0	0	0	0	0	0	133	0	133	0	133
B8	0	0	0	0	0	0	0	0	24	0	24	0	24
B2	0	0	0	0	0	0	0	0	12	0	12	0	12
B2-3	1	1	0	0	0	0	0	0	83	0	83	0	83
B7	0	0	0	0	0	0	0	0	0	0	0	0	0
B5	0	0	0	0	0	0	0	0	21	0	21	0	21
B14	1	1	0	0	0	0	0	0	264	0	264	0	264
B13	0	0	0	0	0	0	0	0	65	0	65	0	65

Figure 6.21*Volume results*

7 Discussions

The technical framework from fault model was gotten from the data collected on the Kilve Beach outcrops, Southwest of England. 18 faults were interpreted between cliff and beach exposures, resulted of a correlation done by fault blocks added in the 3D geological model in Petrel. Below in the *Table 7.1***,** it is shown the number of faults interpreted in the area.

Table 7.1 *Faults interpretation summary*

Faults	Dip Direction	Fault interpretation numbers		
		Cliff	Beach	Both
Normal	North	1	2	10
	South			1
Reverse	North		2	
	South			2

The stratigraphy framework was based on the limestone and shale beddings, they were dipping towards the south following the stratigraphy sequences mapped by Brodahl, E. (1993), and confirmed by the author according to the observations. (*Figure 7.1 and Figure 6.14)*

The fault analysis was done identifying the major faults (according to the measurements and fault trough) and the faults associated to these combined with a view of the fault well exposed on the outcrops in the zone. This combination resulted a better understanding of the structural development of the area. (*Figure 7.2, 5.9 and 6.12 respectively)*

The strike and dip measurements in the faults and beds played an important role in the consistency of the mapping result during the interpretation and understanding the fault behaviour. The measurements and interpretation confirmed that the area is extensional. It confirms the tectonic influence on deposition and stratigraphy framework was described by *Tankard et. al (1989).*

In the mapping a minimum displacement was taken in the F1 (well exposed fault in the locality 1) giving 12 m as result, and recognized as planar fault in initiation stage due to the dip angle 45° (fault initiation are typically in the range 45° and 60° according to Walsh et al., 1991).

Detailed interpretation on the bedding was done taking measurements on the strike, dip and thickness in those places with good exposed and easily access. These values were performed according to their stratigraphy and taken one horizon by block resulted of best matching with the beach exposure photographs, the major number of the point or references acquired by GPS and adding manually where was necessary in order to have more control points to build their surfaces in Petrel.

In Petrel, the 10 most important fault blocks were defined, one was used as boundary on the east of the area, and the fault defined was F15 which was dipping to the south. The beddings were chosen by blocks as well and ideal model built in petrel suggested generate all surfaces as planar due to the inconsistency that could be presented when the dip/strike measurements were loaded in the surface. (*Figure 7.15)*

From the block-0 to block-5, the beding-8 was taken as main horizon where on the upper part seven isochors were generated and in the lower part five isochors were generated. These horizons and isochors were displayed and matched with the photographs. Only one measurement was taken as fault displacement on the field. (*Figure 7.5)*

From the block-7 to block-15, the bedding-11 played as main horizon, generating 9 isochors on the upper part and 3 isochors on the lower part. In terms to build an ideal model, the bedding surfaces were assumed as flat plane (mentioned above) but in the reality were playing the dip and strike over all bedding structures. Taking in account this condition in Petrel, the result was a good matching between the beds and faults (*Figure 7.5, 6.7 and 6.11 respectively).* In addition the beds thickness varies in the reality, the author took an average and saved it in order to generate in Petrel for all the blocks and verify the consistency between them. In general terms, the horizons had a good matching with the photographs taken as base map.

For the fault modelling, they were treated separately due to the different values in dip/strike and direction exposed on the outcrops. The orientation consistency was checked with the faults pillar into the pillar gridding process, also the visualizing if all of them were planar faults adding that some of the small reverse faults interpreted on the reality were not taken into account in the 3D model, only those one were easily to connect manually and finally gave an added value in the

structural development of the area. In the model, effectively the orientation of the faults towards to the north was with striking variable according to the localities; and the orientation of the beds towards to the south; the striking was matched E-W as the interpretations on the field.

Into the 3D model the facies distribution were divided by two models, one with only sand and shale (Model 1- assigned values) and where the facies were mixed as sand fine, sand coarse and shale going through the horizons defined according to the stratigraphy framework generated previously (*Figure 7.18)*. In addition, a connected volume facies was generated in order to see which package of sand or sand bodies were connected between the fault blocks.

The petrophysical properties were taken assigning parameters, varying the porosity beet 0-shales and 25% -sand and permeability between 0 mD shale, 100mD for sand fine and 1000 mD for sand facies.

In the area of the study, it was located a relay ramps, which can be important location for hydrocarbon migration because they link the hanging walls and footwalls of fault systems (Larsen, 1988; Peacock and Sanderson 1994). Flow can occur from the hanging wall, which may be a basin, up the ramp to the footwall. They can be also important location of hydrocarbon traps because of the folding and networks of small-scale faults that occur in ramps (Gawthorpe, R. L., and J. M. Hurst, 1993, Peacock and Sanderson 1994)

This project is a good example where by integrating the data collected in the field, pass through the fault and horizon processes with the objective the create a 3D model that allow to understand the structural behaviour of the locality, and predict or search an approach which could generate the hydrocarbons traps.

8 Conclusions

The Kilve outcrops have been characterized as natural laboratory due to their complexity of the normal fault systems. In the area of the study, it was located a relay ramps which could be used as guideline for hydrocarbons traps prediction. The relay ramps can reorient strata that connect the hanging wall and footwall of normal fault system. The strike and dip measurements in the faults and beds played an important role in the consistency of the mapping result during the interpretation and understanding the fault behaviour. The measurements and interpretation confirmed that the area is extensional

The Kilve Beach area is dominated lithologically by mudstones and interbedded with limestones beds. From Observations in the locality 3 we can say that the Early Jurassic Blue Lias Formation is dominated structurally by WNW trending. Tthickness of the beds increase towards to eastern (Early Lias formations)

The stratigraphy framework was based on the limestone and shale beddings, they were dipping towards the south following the stratigraphy sequences mapped by Brodahl, E. (1993), and confirmed by the author according to the observations.

18 faults were interpreted on the outcrops and 11 faults (8 were interpreted as normal and 3 as reverse) were included in 3D geological model using *Petrel* ™ software (small reverse faults and those exposed only in the cliff section were exclude), in addition, 13 horizons were generated taking in account the stratigraphic sequences. The fault and horizons gave a good matching on the photographs digitized and with the interpretations done in the field.

Facies and petrophysical properties were added given as result volume calculation simulating a gas field (*GIIP (in gas) = 668[*10^6 sm3]*)

9 Recommendations for further work

Increase the density of data collected by km^2 in order to improve the resolution of the model.

Extend the study area to the surrounding of Kilve Beach, and integrate the seismic, logs and petrophysics interpretations available from the area.

Include a facies approach in the fault zone with high content of fractures, where the vertical component plays an important role providing certain constrain in 3D geological model.

Build a reservoir simulation model by using data from the North Sea fields. The simulation model should include sensitivities in order to correlate the faults modeled and the transmissibility computed by the reservoir simulator. This is especially important because of the large number of fields in the North Sea which its developments are linked to the fault behavior.

10 References

Antonellini M., Aydin A., 1994, Effect of faulting on fluid flow in porous sandstones: petrophysical properties: The American Association of Petroleum Geologists Bulletin, v. 78, p 335–377

Bartley, J. M., and A. F. Glazner, 1991, En echelon Miocene rifting in the southwestern United States and model for vertical-axis rotation in continental extension: Geology, v. 19, p. 1165–1168

Beach, A., 1989 the geometry of normal faults—examples from the Jurassic of Somerset (abs.): Geological Society of London Meeting, The Geometry of Normal Faults, London, June 14–15.

Bowyer, M.O.N., and Kelly, P.G. 1995. Strain and scaling relationships of faults and veins in Kilve, Somerset . Proceeding of the Ussher Society, v.8, p 411-416.

Brodahl, E. (1993). Fault Pattern in nord Somerset . Unpublished thesis for candidature of Geology and rocks mechanics . University of Trondheim, 72 p .

Caine, J. S., James, P. E. & Forster, G. B., 1996. Fault zone architecture and permeability structure. Geology 24 (11), p 1025-1028.

Cornford, C.,1986, The Bristol Channel Graben: organic geochemical limits on subsidence and speculation on the origin of inversion. Proceeding of the Ussher Society, v.6, p 360-367.

Cornford, C.,2003, Triassic palaeo-pressure and Liassic mud volcanoes near Kilve, West Somerset. Geoscience in south-west England, v.10, p 430-434.

Cox, B.M., Sumbler, M.G. & Ivimey-Cook, 1999. A formational framework for the Lower Jurassic of England *and Wales (on shore area)*. BGS research report RR/99/01

Edwards, R.A., 1999, The Minehead district—a concise account of the geology, Memoir for 1:50,000 Geological Sheet 278 and part of sheet 294 (England and Wales). British Geological Survey, the Stationery. Office, London.

Engelder, T. and Peacock D. C. P. 2001. Join development normal to regional compression during flexure-flow folding: the Lilstock buttress anticline, Somerset, England. Journal of Structural Geology 23, p 259-277

Fredman, Niclas; Tveranger, Jan; Cardozo, Nestor; Braathen, Alvar; Soleng, H. H.; Røe, P.; Skorstad, A.; Syversveen, A. R.; 2008. Fault facies modelling; technique and approach for 3D conditioning and modelling of faulted grids AAPG Bulletin 92, no. 11, p. 1457-1478.

Gawthorpe, R. L., and J. M. Hurst, 1993, Transfer zones in extensional basins: their structural style and influence on drainage development and stratigraphy: Journal of the Geological Society of London, v. 150, p. 1137–1152.

Glen, R.A., hancock, P.L. and Wittaker, A., 2005, Basin inversion by distributed deformation: the southern margin of the Bristol Channel Bassin, England: *Journal of Structural Geology*, v.27, p 2113-2134.

Jones, G., Fisher, Q.J., and Knipe, R.J., eds., 1998,Faulting, Fault Sealing and Fluid Flow inHydrocarbon Reservoirs: Geological Society of London Special Publication 147, 319 p.

Kamerling, P. 1979. The geology and hydrocarbon habitat of the Bristol Channel Basin. Journal of Petroleum Geology 2 (1), p 75-93.

Kelly, P.G., 1998. Development and Interaction of Segmented Fault Systems. Unpublished Ph.D. thesis, University of Southampton, 167 p.

Kim, Y.S., Peacock D. C. P., Sanderson D. J. 2004. Fault damage zones. *Journal of Structural Geology*, v.26, p 503-517.

Knipe R. J., Fisher Q. J., Jones G., 1997.In Hydrocarbon Seals: Importance for Exploration and Production, Fault seal analysis: successful methodologies, application and future directions, NPF Special Publication, eds Moller-Pedersen P., Koestler A. G. 7, p 15–40

Knott S. D. 1993 Fault seal analysis in the North Sea. American Association of Petroleum Geologists Bulletin 77, p 778–792

Larsen, P.-H., 1988. Relay structures in a Lower Permian basement- involved extension system, East Greenland: Journal of Structural Geology, v. 10, p. 3–8.

Lindanger, M., 2003. A study of rock lenses in extensional faults, focusing on factors controlling shapes and dimensions. Unpublished thesis for Candidatus Scientiarum degree. University of Bergen, 166 pp.

Mandl, G., 1988. Mechanics of tectonic faulting: Models and basics concepts, Amsterdam, Elseiver, 407 p

Masson, D.G., and P.R. Miles, 1986a, Development and hydrocarbon potential of Mesozoic sedimentary basins around margins of North Atlantic: American Association of Petroleum Geologists Bulletin, v. 70, p. 721-729.

Millson, J., 1987, The Jurassic evolution of the Celtic Sea basins, in J. Brooks and K.W. Glennie, eds., Petroleum geology of North West Europe: London, Graham and Trotman, p. 599-610

Palmer, C.P. 1972. The Lower Lias (Lower Jurassic) between Watchet and Lilstock in North Somerset (United Kingdom). Newsletter of Stratigraphy, v.2, p 1-30.

Peacock D. C. P., Sanderson D. J. 1994. Geometry and development of relay ramps in normal fault systems. American Association of Petroleum Geologists Bulletin 78, p 147–165.

Peacock D. C. P., Sanderson D. J. 1995. Strike-slip ramps. Journal of Structural Geology, v.7, p 1351-1360

Peacock D. C. P., Sanderson D. J. 1999. Deformation history and basin-controlling faults in the Mesozoic sedimentary rocks of Somerset coast. Proceeding of the Geological Association, 110, p 41-52.

Roberts, A.M, Yielding, G., and Freeman, B., 1991. The geometry of normal faults. Journal of the Geological Society, London, Special Publications v.147, p. 185-187.

Simms, M.J., Chidlaw, N., Morton, N. & Page, K.N., 2004, British Lower Jurassic Stratigraphy, Geological Conservation Review Series, No. 30, Joint Nature Conservation Committee, Peterborough, 458 p

Steen Øyvind, 1995. Field observations to test methods for identification of faults using dipmeter logs; examples from Kilve in South England. Reservoir Techn. Report. 17 p

Tankard, A.J. and Balkwill, H.R. 1989. Mesozoic History of the Celtic Sea Basins: Chapter 28: Extensional Tectonics and Stratigraphy of the North Atlantic Margins. Tulsa, American Association of Petroleum Geologists . p 433-444

Tappin, D.R., Ciiadwick, R.A., Jacson, A.A., Wingfielo, R. T.R and Smith, N.J.P., 1994.The Geology of Cardigan Bay and The Bristol Channel. United Kingdom Offshore Regional Report. British Geology Survey.

Townsend, C., Firth, I., Westerman, R., Kirkevollen, L., Harde, M., Andersen, T., 1998. Small seismic-scale fault identification and mapping, In: Jones, G., Fisher, Q.J., Knipe, R.J. (Eds.), Faulting, fault sealing and fluid flow in hydrocarbon reservoirs. Geological Society, London, Special Publications, pp. 1-25.

Van der Zee W., Urai J.L., 2005. Processes of normal fault evolution in a siliciclastic sequence: a case study from Miri, Sarawak, Malaysia. Journal of Structural Geology 27, p. 2281–2300

Van Hoorn, B., 1987, The South Celtic Sea/Bristol Channel basin: origin, deformation and inversion history, in P.A. Ziegler, ed., Compressional intraplate deformations in the Alpine foreland: Tectonophysics, v. 137, p. 309-334.

Walsh J. J., Watterson J. 1992. Populations of faults and fault displacements and their effects on estimates of fault-related regional extension. Journal of Structural Geology 14, p 701–712

Walsh J. J., Watterson J. (1991) in The Geometry of Normal Faults, Geometric and Kinematic coherence and scale effects in normal fault systems, Geological Society, London, Special Publications, eds Roberts A. M., Yielding G., Freeman B. 56, p 193–203

10.1 Maps References

Quantock Hills and Bridgwater maps -1:25000 scale digitized in ANQUET MAPS 2011 (a program commercially available on the Ordnance Survey in UK)

10.2 Manual references

Petrel Geology course. 2011. Schlumberger.

11 Appendix

11.1 Raw data collected-GPS points

Table 11.1 *GPS points collected in the area according to the fault block*

NAME	X	Y	Fault Block
F1	484267,481	5671435	1
F1D	484261,55	5671437,91	1
F2C1	484330,007	5671406	2
F2D	484310,157	5671450,66	2
F2D1	484323,92	5671449,51	2
F2D2	484340,89	5671445,67	2
F2L9	484228,624	5671456,69	2
F3D1-	484348,435	5671444,87	3
F3D2-	484370,515	5671444,25	3
F3D3-	484383,99	5671440,09	3
F3L6A	484333,069	5671447,48	3
F3L6AB	484326,991	5671448,27	3
F3L7A	484322,456	5671450,4	3
F3L7AB	484318,053	5671450,53	3
F3L8A	484310,511	5671451,99	3
F3L8AB	484302,826	5671452,91	3
F3L9U	484258,199	5671461,83	3
F3U	484450,828	5671450,46	3
F4D1	484508,938	5671463,07	4
F4D2	484494,483	5671466,56	4
F4D3L9	484473,312	5671467,63	4
F4D4L10	484450,753	5671471,81	4
F4D5L10&	484419,035	5671474,46	4
F4D6L10	484389,347	5671478,11	4
F4DL1	484514,322	5671464,05	4
F4L2	484501,69	5671469,43	4
F4U	484543,756	5671468,86	4
F5end	484515,114	5671471,95	5
F5L1	484527,137	5671473,02	5
F5U	484582,746	5671490,76	5
F6U	484598,561	5671498,17	6
F6U2	484613,27	5671509,35	6
F7AL2	484554,451	5671516,2	7
F7BL1	484567,29	5671486,58	7
F7D	484595,488	5671545,33	7
F7D1	484588,926	5671547,35	7
F15-1	484706,862	5671610,61	14
F15-2	484725,954	5671615,67	14
F15-3	484737,697	5671616,64	14
AftRH	484902,1	5671578	13
AftRH2	484915,3	5671592	13
AftRH3	485006,5	5671641	13
AftRH4	485052,5	5671706	15
AftRH5	485079,8	5671741	15
DC1L8	484224,3	5671434	1
DC2L6	484245,7	5671435	1
DC3L3	484270,6	5671433	1
DC4L4	484292,6	5671435	1
DC5L4	484304	5671437	5
DC6L3	484330,4	5671430	7
L10D1	484253,2	5671454	1
L10D10	484540,8	5671484	1
L10D11	484541,4	5671489	1
L10D2	484281,7	5671462	1
L10D3	484322,7	5671469	1
L10D4	484349	5671468	1
L10D5	484405,4	5671468	1
L10D6	484460,2	5671461	1
L10D7	484479,7	5671462	1
L10D8	484505,6	5671459	1
L10D9	484525,1	5671456	1
L10F6-1	484540,4	5671481	1
L10Rev	484567,7	5671494	1
L11-1	484228,2	5671457	1
L11F1AR	484193,6	5671446	1
L11F2ARR	484198,2	5671447	1
L11F3AB	484255,9	5671457	2
L11F3AR	484259	5671458	2
L11F6	484529	5671488	5
L11F6B	484539,2	5671484	5

11.2 Fault data collected on the cliff section.

Table 11.2 *Dip and strike values taken in the cliff section*

Fault name	*Dip Angle*	*Direction*
F1	43N	N15W
CLIFF3		
F2	61N	N12W
F3	52N	N55W
F4-A	43N	N15W
F4	43N	N75W
F5	61N	N10W
F7	48N	N20W
F8-A	20N	N10E
F8	68N	N10W
F9	89NE	N2W
F10	76N	N5W
F12	65N	N3W
F13	89N	N5W
F14	47S	N3W